LAWRENCE
LIVERMORE
NATIONAL
LABORATORY

LLNL-TR-516874

Contract B590089: Technical Evaluation of the Pu Cluster Calculations

J. G. Tobin, M. Ryzhkov, A. Mirmelstein

November 29, 2011

Disclaimer

This work performed under the auspices of the U.S. Department of Energy by Lawrence Livermore National Laboratory under Contract DE-AC52-07NA27344.

Contract B590089: Technical Evaluation of the Pu Cluster Calculations

Primary Author: J.G. Tobin, LLNL, Tobin1@LLNL.Gov, x27247

Contributing Authors: Michael Ryzhkov, Russian Academy of Science, Ekaterinburg, Russia

Alex Mimrelstein, Russian Federation Nuclear Lab, VNIITF, Snezhinsk, Russia

Abstract

Using Synchrotron-Radiation-based Photoelectron Spectroscopy and X-ray Absorption Spectroscopy, the theoretical results within recent progress reports supplied under Contract B590089 have been evaluated. Three appendices are included: A is from Progress Report I; B is from Progress Report II; and C is from an earlier calculation by M. Ryzhkov. The comparisons between the LLNL experimental data and the Russian calculations are quite favorable. The Cluster calculations may represent a new and useful avenue to address unresolved questions within the field of actinide electron structure, particularly that of Pu.

The experimental results have been extracted from earlier publications by LLNL personnel. These are listed below.

References

1. J.G. Tobin and S.-W. Yu, Phys. Rev. Lett, **107,** 167406 (2011).
2. S.-W. Yu, J. G. Tobin, J. C. Crowhurst, S. Sharma, J. K. Dewhurst, P. Olalde-Velasco, W. L. Yang, and W. J. Siekhaus, Phys. Rev. B **83**, 165102 (2011).
3. J.G. Tobin, B.W. Chung, R. K. Schulze, J. Terry, J. D. Farr, D. K. Shuh, K. Heinzelman, E. Rotenberg, G.D. Waddill, and G. Van der Laan, Phys. Rev. B **68**, 155109 (2003).
4. J.G. Tobin, P. Söderlind, A. Landa, K.T. Moore, A.J. Schwartz, B.W. Chung, M.A. Wall, J.M. Wills, R.G. Haire, and A.L. Kutepov, J. Phys. Cond. Matter **20**, 125204 (2008).
5. S.-W. Yu, J. G. Tobin, P. Olalde-Velasco, W. L. Yang, and W. J. Siekhaus, "Energy Calibrations in the X-ray Absorption Spectroscopy of Uranium Dioxide," J. Vac. Sci. Tech. A, accepted, Nov 2011.

Comparison 1: X-ray Photoelectron Spectroscopy (XPS), Bremstrahlung Isochromat Spectroscopy (BIS), also known as Inverse Photoelectron Spectroscopy (IPES), and X-ray Absorption Spectroscopy (XAS) versus cluster calculation results for UO_2.

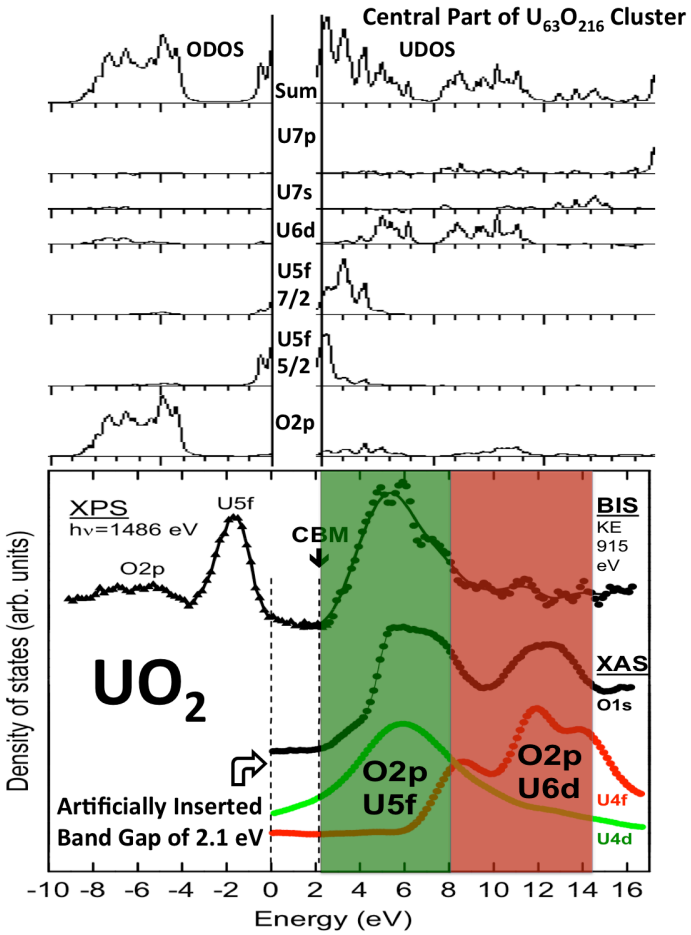

The experimental results (bottom) are from References 1 and 2 and the theoretical results (top) are from Appendix C.

This is very promising. Because we inserted a band-gap of 2.1 eV artificially, the density of states (DOS) calculations have been split at the energy zero and aligned with the valence band maximum (VBM) in the XPS and the Conduction Band Minimum (CBM) in the BIS and XAS. UDOS is the unoccupied density of states. ODOS is the occupied density of states. While others have already made such comparisons with XPS and the ODOS [Y.A. Teterin and A.Y. Teterin, Russian Chemical Reviews 73, 541 (2004)], this is the first such definitive comparison of the ODOS with the BIS and XAS. In general, there is strong agreement in terms of the U6d, U5f, and O2p DOS with the spectral features.

Comparison 2: Synchrotron-Radiation-based Photoelectron Spectroscopy (PES) versus cluster calculation results for PuO_2.

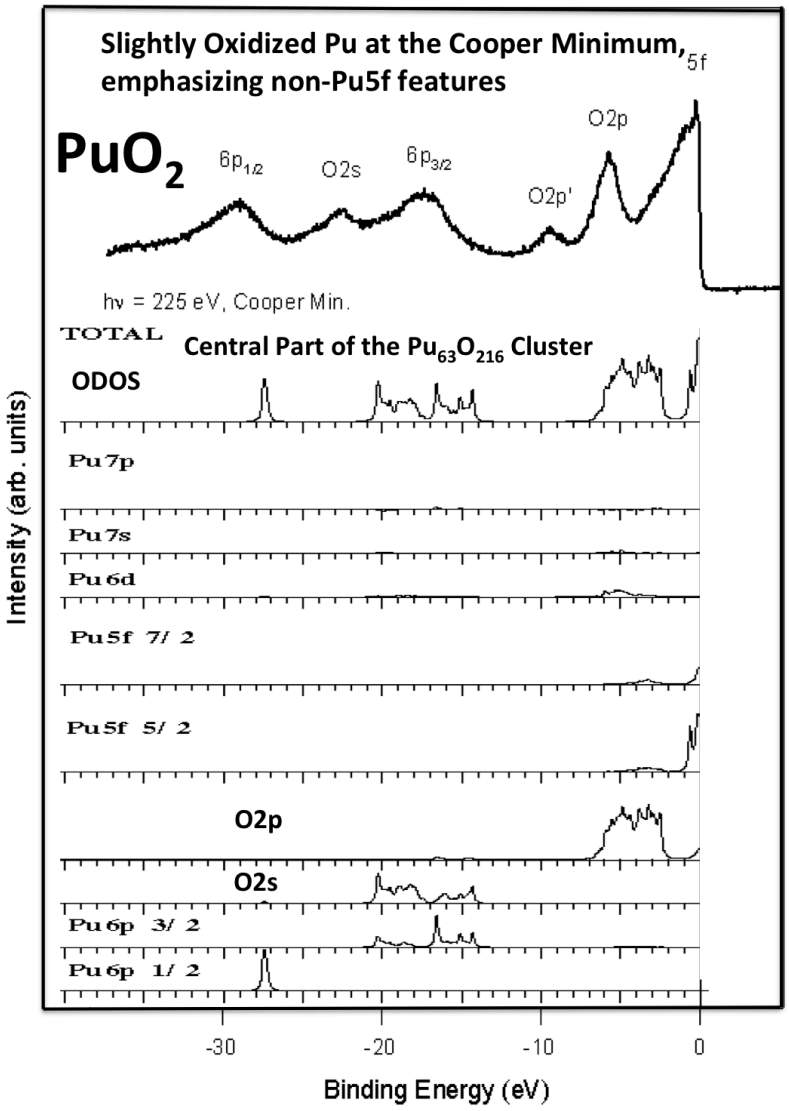

The experimental results (top) are from Reference 3 and the theoretical results (bottom) are from Appendix C. This Pu spectrum are from an alpha-Pu sample with a delta-Pu surface reconstruction.

By working at the Cooper Minimum, the relative intensity of the Pu 5f can be diminished and the contribution of the other peaks amplified. Clearly, there is once again strong agreement between the ODOS for the Pu5f, O2p, Pu6p3/2, O2s, and Pu6p1/2 and the corresponding spectroscopic features.

Comparison 3: Synchrotron-Radiation-based Photoelectron Spectroscopy (PES) versus cluster calculation results for Pu.

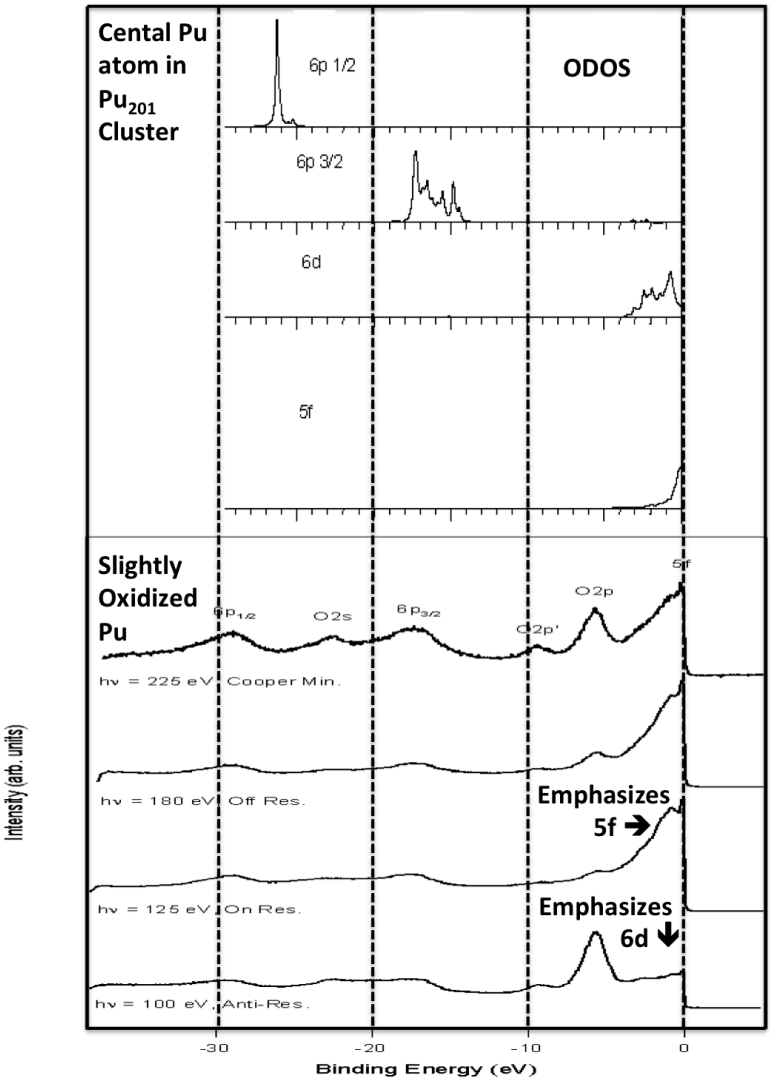

The experimental results (bottom) are from Reference 3 and the theoretical results (top) are from Appendix B. These Pu spectra are from an alpha-Pu sample with a delta-Pu surface reconstruction.

The calculations once again provide a meaningful simulation of the observed states: Pu5f, Pu6d, Pu6p3/2 and Pu6p1/2. By tuning the photon energy, different states can be emphasized and de-emphasized. At the anti-resonance, hv = 100 eV, the Fermi Edge step should be representative of the Pu 6d states. On Resonance, hv = 125 eV, the Fermi Edge should be dominated by the Pu5f states. Despite the small amount of oxidation, these spectra should provide accurate basis for comparison with bulk, metallic Pu.

Comparison 4: 5f occupations.

	basis	Pu_1 site	Pu_2 site
Pu_2 dimer (R = 3.28 Å)	minimal		
	extended	$5f^{5.80}6d^{0.98}7s^{1.04}7p^{0.18}$	
Pu_{19} cluster	minimal	$5f^{5.15}6d^{2.55}7s^{0.40}$	
	extended	$5f^{5.48}6d^{3.22}7s^{0.08}7p^{-0.54}$	
Pu_{79} cluster	minimal	$5f^{5.20}6d^{2.02}7s^{0.23}$	$5f^{5.38}6d^{2.65}7s^{0.38}$
	extended	$5f^{5.51}6d^{2.68}7s^{0.30}7p^{-0.24}$	$5f^{5.51}6d^{2.84}7s^{0.22}7p^{-0.27}$
Pu_{201} cluster	minimal	$5f^{4.92}6d^{3.60}7s^{0.47}$	$5f^{5.11}6d^{3.95}7s^{0.47}$
	extended	$5f^{5.17}6d^{3.79}7s^{0.45}7p^{0.58}$	$5f^{5.41}6d^{3.83}7s^{0.47}7p^{-0.35}$

JPCM
Exp
Estimates

Bulk Pu
5f $^{5.1\pm0.1}$

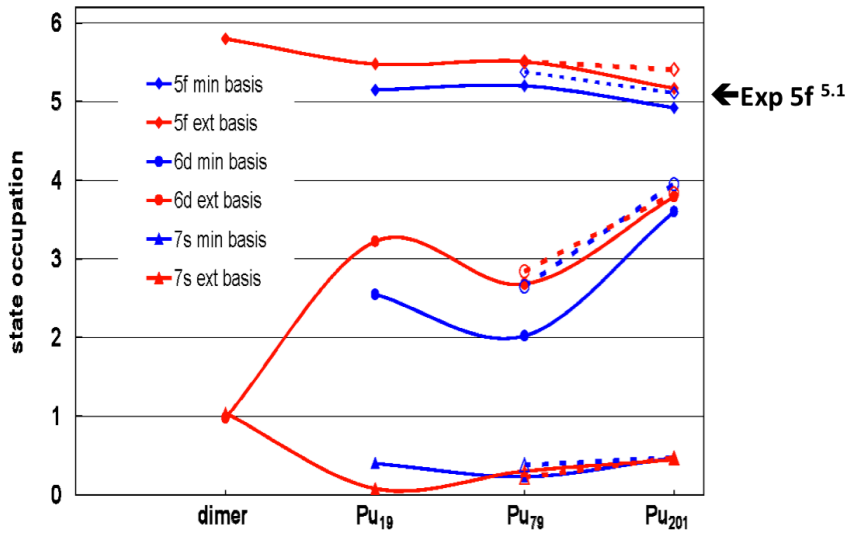

One of the crucial issues in Pu electronic structure is that of the differentiation of the 6d and 5f states. Where are the Pu5f and Pu 6d states? What are their occupations? An intriguing and potentially powerful avenue of addressing this problem may be through the cluster calculations. The results of the cluster calculations shown here suggest that it may be possible to follow the development of these orbitals as a function of size. It is important that the largest cluster converges to good approximation with the experimentally determined bulk Pu5f occupation. A brief summary of the spectroscopic justification for this determination is shown on the next page.

This is a summary of our earlier results from Reference 4, with the inset in the top panel being taken from Reference 5.

The absence of the pre-peak in the 5d XAS and the tremendous diminishment of the Pu4d3/2 peak relative to the Pu4d5/2 peak are both strong indications that the occupation of the Pu5f states must be very near to 5. For a complete description of these arguments, please see reference 4.

The Pu4d spectrum is from an alpha-Pu sample with a delta-Pu surface reconstruction.

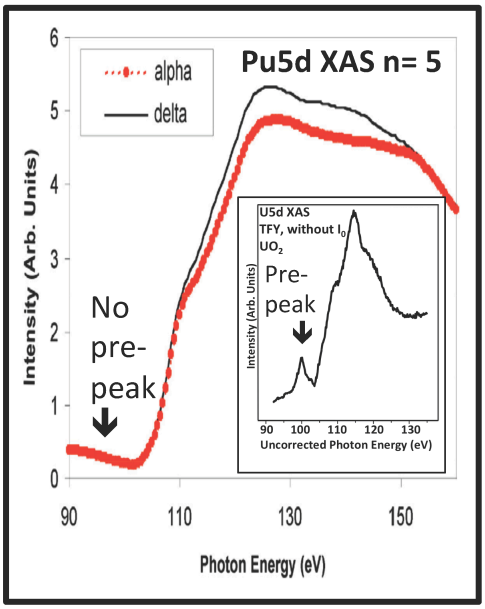

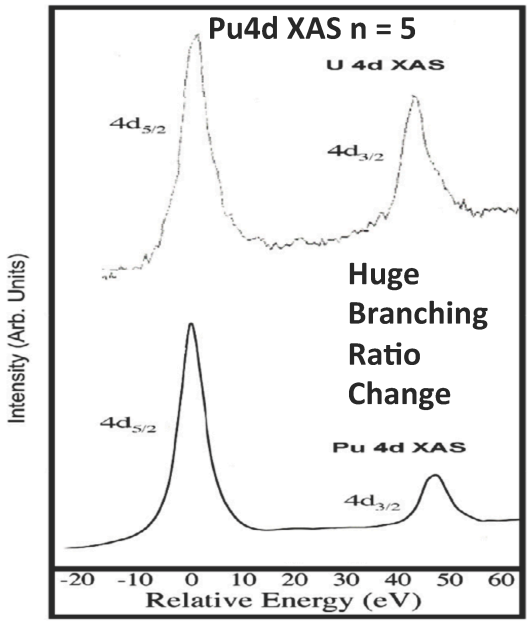

There are strong indications that the cluster calculation approach may provide us with substantial and new insight into the nature of the electronic structure of bulk, metallic Pu.

Federal State Unitary Enterprise
"Russian Federal Nuclear Center – Zababakhin All-Russia Research Institute of Technical Physics"
FSUE "RFNC-VNIITF"

REPORT ON DETAILS OF FIRST AND SECOND QUARTER RESULTS

Material Support Agreement No. B590089

"Electronic structure of actinide dimers and Pu_{19} cluster. Training high-pressure X-ray diffraction experiments"

Snezhinsk 2010

Content

Abstract

Quantum-chemical calculations of electronic structure and chemical bonding of actinide (An) dimers were performed on the basis of cluster approach. Geometry optimization of An_2 molecules for all actinides from Th to Lr was performed using the well-known quantum-chemical technique $DMol^3$ in the scalar relativistic approach and the double numerical atomic basis set. Full potential linearized augmented plane waves (FLAPW) method was applied to verify the equilibrium distances and binding energies for Np_2, Pu_2, Am_2, and Cm_2 dimers obtained by $DMol^3$ technique. It is shown that all the members of actinide series from Th to Lr can form bonded dimers. Light actinides (Th to U) form "strongly bonded" dimers, dimers of heavy actinides (Cm to No) turn out to be "weakly bonded" whereas Np, Pu, and Am are found to lie within a crossover region between strongly and weakly coupled dimers.

Our results show that significant decrease of binding energies in the heavy part of An_2 series is not simply due to the localization of 5f states, since the contribution of 5f atomic orbitals to bonding even in Np_2 (with quite high atomization energy and short bond length) is quite small as compared to the role of 6d, 7s and 7p states. However, the investigation of plutonium dimer with various equilibrium distances reveals the 5f-5f and 5f-6d interactions to be extremely sensitive to the molecular size.

Investigations of the plutonium dimer and 19-atom cluster corresponding to δ-Pu predict noticeable hybridization of Pu5f states with 6d orbitals of nearest metal sites as well as with 5f atomic orbitals of the nearest neighbors in the molecule or in the crystal lattice. Due to this hybridization the number of 5f electrons could be quite different in the simple dimer (N_f = 5.8) and in the system with high coordination of metal atom (N_f = 5.15 or 5.48).

A set of test and training X-ray diffraction experiments under high pressure was performed using STOE IPDS II diffraction system with imaging plate detector and Almax-Boehler diamond anvil cell. In these experiments we were able to observe the isostructural pressure-induced $\gamma \rightarrow \alpha$ phase transition in the metallic cerium and to estimate the change in volume the value of which was found to be very close to the literature data. Also, the existence of pressure-induced room temperature structural phase transition in intermetallic compound CeNi was confirmed.

The results of the test and training experiments demonstrate that the RFNC-VNIITF diffraction group has learned to carry out elementary operations to prepare samples and DAC for high-pressure X-ray diffraction measurements and has gained initial experience of performing such experiments. At the same time, it is evident that the technological level of these experiments requires further improvements.

I. Theoretical part. The RDV cluster calculations of the electronic configuration of face-centered cubic plutonium metal.

Introduction

The nature of ground state of metallic plutonium is one of the central problems in modern solid state physics. In spite of the considerable progress in the field of both theory and experiment, many questions regarding the physics of plutonium metal remain unanswered, including those concerning the number of electrons in its f shell, understanding of its magnetic properties, and the driving forces of structural phase transition in plutonium. The analysis of X-ray absorption spectra and the results of electron energy losses spectroscopy [1] show that the number of electrons in 5f-shell N_f is near 5.2 in both α- and δ-Pu. Similar value of N_f was also obtained in DMFT calculations by Shim et al. [2]. However, the description of the magnetic susceptibility and specific heat of plutonium based on the multiple intermediate valence (MIV) approach shows that N_f is less than 5 in both Pu phases. It is evident that there are serious shortcomings in both approaches. The many-electron model used for the analysis of X-ray and electron absorption spectra is formally appropriate for isolated atoms. On the other hand, the empirical MIV model is also some simplification since it uses the expressions of "ordinary" fluctuating systems with intermediate valences. Thus this model also needs verification and development.

The general aim of the present work is quantum-chemical investigation of electronic structure and chemical bonding in plutonium metal based on the cluster approach. These calculations can provide a more fundamental understanding of the transformation of plutonium atomic configuration when going from an isolated atom to a molecular system and to a solid. Another aim of the work is independent evaluation of the number of 5f electrons in δ-Pu.

According to the Statement of Work, the work to be performed during the first half-year of the Contract execution includes *i*) investigation of the fully relativistic electronic and chemical bonding structures as well as electronic configuration of atoms in actinide dimers and *ii*) investigation of the chemical bonding structure and atomic orbital (AO) populations for the central Pu atom in Pu_{19} cluster which geometry and boundary conditions correspond to the face-centered cubic δ-Pu lattice.

Molecular systems containing actinides such as actinide dimers An_2, i.e. the simplest molecular systems, became the subject of experimental [4] and theoretical studies [5,6] quite recently. The earlier quantum chemical investigations used the non-relativistic scattered wave

(SW) method, single-reference-configuration-interaction method (SRCI), Hartree-Fock method (HF) with relativistic core potential and configuration interaction included. Bursten and co-workers [5] assumed that two potential energy minima at 3.0 and 2.2 Å exist for U_2 and Np_2. The authors of [6] investigated Pu_2 molecule and found that its dissociation energy and equilibrium distance are near 0.3 eV and 4.5 Å, respectively. The aim of the first step of present work is the search for all possible hypothetical actinide dimers from Th_2 to Lr_2, detailed investigation of chemical bonding, and the role of 5f electrons in Np_2, Pu_2 and Am_2 molecules. The Pu_2 chemical bonding transformation will also be studied for the case when Pu–Pu bond length decreases from 4.5 Å (isolated molecule) to 3.28 Å (δ-Pu) and 2.6 Å (α-Pu).

I.1. Methods of calculations

Geometry optimization of An_2 molecules for all actinides from Th to Lr was performed using the DMol^3 method [7] in the scalar relativistic approach [8,9] and double numerical atomic basis set ("dnd"). The generalized gradient approximation (GGA) in Perdew-Burke-Ernzerhof ("PBE") [10] and Becke-Lee-Yang-Parr ("BLYP") [11] forms was used in all the calculations. Optimization of the molecular structures proceeded until the change in a value of maximum energy gradients did not become less than 0.001 atomic units. To verify the scalar relativistic DMol^3 results we also used the FLAPW (full potential linearized augmented plane waves) method [12] in the version of WIEN2k package to obtain the equilibrium distances and binding energies for Np_2, Pu_2, Am_2, and Cm_2 dimers. The latter calculations were performed with the "PBE" functional taking into account the spin–orbit coupling.

To investigate the nature of chemical bonding and the role of 5f electrons in Np_2, Pu_2, and Am_2 we also used the fully relativistic discrete variational method (RDV) [13,14]. For each final bond length obtained by DMol^3 and FLAPW, the RDV calculation was carried out. The RDV method is based on the solution of the Dirac-Slater equation for 4-component wave functions transforming according to the irreducible representations of the double point groups ($D_{\infty h}$ in the present calculations). For the calculation of symmetry coefficients we used the original code which realizes the projection operators technique [13] and includes the matrices of irreducible representations of double point groups obtained in Ref. [15] aw well as the transformation matrices presented in Ref. [16]. The extended bases of 4-component numerical atomic orbitals (AO) obtained as the solution of the Dirac-Slater equation for the isolated neutral atoms also included An$7p_{1/2}$ and $7p_{3/2}$ functions in addition to the occupied AOs.

I.2. Electronic structure of actinide dimers

Table 1 presents the results of geometry optimization of actinide dimers using DMol and FLAPW methods. As can be seen, the "PBE" functional in DMol approach noticeably shifts the absolute values of binding energy $|E_b|$ (which is sometimes called the atomization energy) upward for the light actinides from Th_2 to Pu_2 but considerably underestimates E_b for Am_2 and Cm_2 as compared to "BLYP" calculations. The bond lengths R_e obtained in FLAPW calculations have the same trend, however R_e for Np_2 and Cm_2 exceeds by 0.4 Å the nearest value in DMol results. The values of E_b obtained in FLAPW calculations have also the same trend as the results of DMol and in all cases fall between the energies correspondent to "PBE" and "BLYP" functionals in DMol technique. The variations of calculated $-E_b$ and equilibrium distances R_e are shown in Fig. I.1. The values of binding energies strongly correlate with equilibrium distances for almost all dimers, i.e. the more short An – An bonds correspond to the higher atomization energies. Cm_2 is the only exception from this rule, since the decrease of its R_e on ~ 1 Å as compared to the neighboring Am_2 and Bk_2 is not accompanied by the corresponding growth of

Table 1. Energies (eV) and bond lengths (Å) for actinide dimers.

Dimer	DMol[3]				FLAPW	
	PBE		BLYP			
	E_b	R_e	E_b	R_e	E_b	R_e
Th_2	-5.31	2.69	-4.46	2.77		
Pa_2	-4.88	2.60	-4.03	2.75		
U_2	-5.37	2.94	-3.93	3.13		
Np_2	-5.49	3.02	-4.62	3.33	-5.06	3.70
Pu_2	-1.79	4.53	-0.76	5.16	-1.23	4.42
Am_2	1.13	5.03	-0.76	5.34	0.12	4.72
Cm_2	0.29	4.01	-0.90	4.28	-0.73	4.68
Bk_2	-1.15	4.86	-1.17	5.24		
Cf_2	-1.32	4.85	-1.42	5.31		
Es_2	-1.48	4.65	-1.41	5.07		
Fm_2	-1.44	4.45	-1.42	4.67		
Md_2	-1.24	4.28	-1.28	4.42		
No_2	-0.04	5.01	-0.27	5.58		
Lr_2	-4.74	3.47	-4.38	3.61		

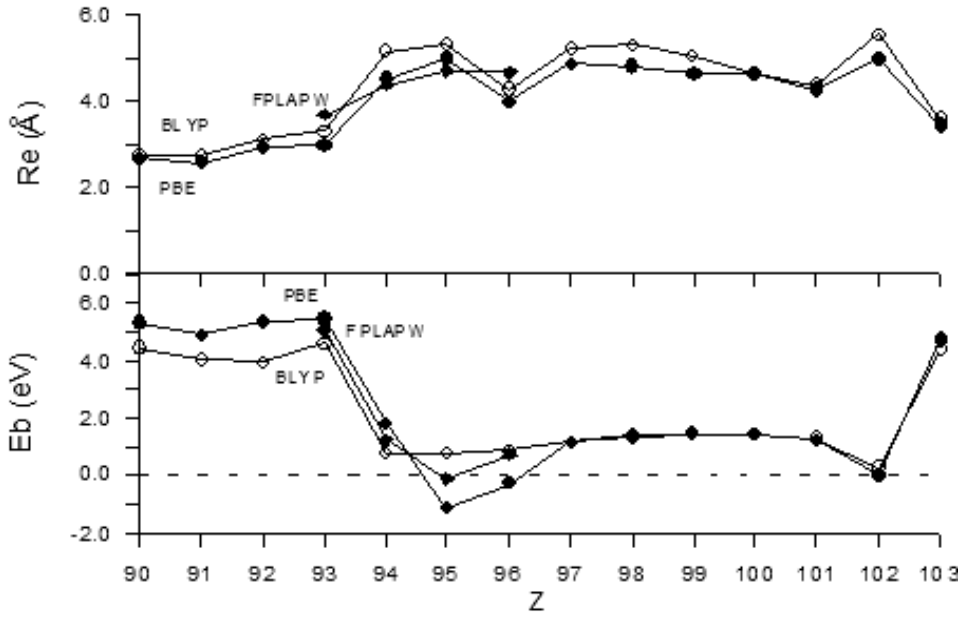

Figure I.1. The binding energy and bond length as a function of atomic number Z for actinide An_2 molecules. Signs correspond to the results obtained by different calculation techniques, i.e. "BLYP" (open circles), "PBE" (black circles), and "FLAPW" (black rhombs).

binding energy. It should be noted, that both DMol and FLAPW formalisms predict the bonded ground states for almost all dimers as well as rather large equilibrium distances for molecules from Pu_2 to No_2.Using different theoretical methods Archibong and Ray found also large R_e for Pu_2 between 4.38 and 4.5 Å [6]. The "PBE" functional in our DMol and FLAPW calculations predicts the nonbonding ground states for Am_2 and Cm_2, however, according to the calculations with "BLYP" exchange-correlation potential, both dimers are weakly bonded. On the other hand, the "BLYP" functional predicts rather weak bonding for Pu_2 (-0.76 eV) as compared with -1.79 eV obtained with "PBE" approach. Archibong and Ray found for Pu_2 even smaller dissociation energy, between 0.24 and 0.38 eV [6].

As seen in Fig. I.1, the actinide dimers form two groups of chemically different molecules: the so-called "strongly bonded" (Th_2 to Np_2 and Lr_2) and "weakly bonded" (Am_2 to No_2). Np_2, Pu_2 and Am_2 could be considered as a "transition" between these groups. This transformation of chemical bonding needs a more detailed investigation which can be done on the base of LCAO description (linear combination of atomic orbitals) of molecular orbital (MO) structure. The fully relativistic RDV method may serve this purpose.

Since different theoretical formalisms predict R_e for Pu_2 to be close to 4.5 Å, a first step of RDV investigation of Pu_2 was carried for this equilibrium distance. The total and partial densities of states (DOS) obtained for the Pu_2 molecule in RDV calculation are shown in Fig. I.2. During the construction of theoretical DOS from MO structure, we have broadened each MO level by a Lorentzian function of the constant width for all MOs. Since the partial DOS for

$Pu7p_{1/2}$ and $7p_{3/2}$, $6d_{3/2}$ and $6d_{5/2}$, $5f_{5/2}$ and $5f_{7/2}$ are close to each other, the total DOS for 7p, 6d and 5f MOs are presented in the figure.

The energy level structure obtained for Pu_2 is quite typical for heavy metal compounds. The occupied valence molecular states contain main contributions from Pu7s and $5f_{5/2}$ AOs, the vacant MOs are formed by $Pu5f_{7/2}$, 6d and 7p orbitals. The energy gap obtained in our relativistic calculations for Pu_2 is near 0.9 eV. The highest occupied molecular orbital (HOMO) contains 88% of 7s AO with small admixtures of $5f_{5/2}$, $7p_{3/2}$, and $6d_{5/2}$ states. The lowest unoccupied molecular orbital (LUMO) is of almost purely (97%) $5f_{7/2}$ character. The HOMO and LUMO correspond to S1U and S3U irreducible representations of $D_{\infty h}$ double point group, respectively (the notations of representations correspond to Ref. [17]). The spin-orbital interaction is small for 5f, 6d, and 7p levels, particularly the ~1 eV splitting of the Pu5f band (Fig. I.2) is due to this interaction. However, similar ~ 1 eV splitting of the S1U and S1G types of 7s levels (Fig. I.2)

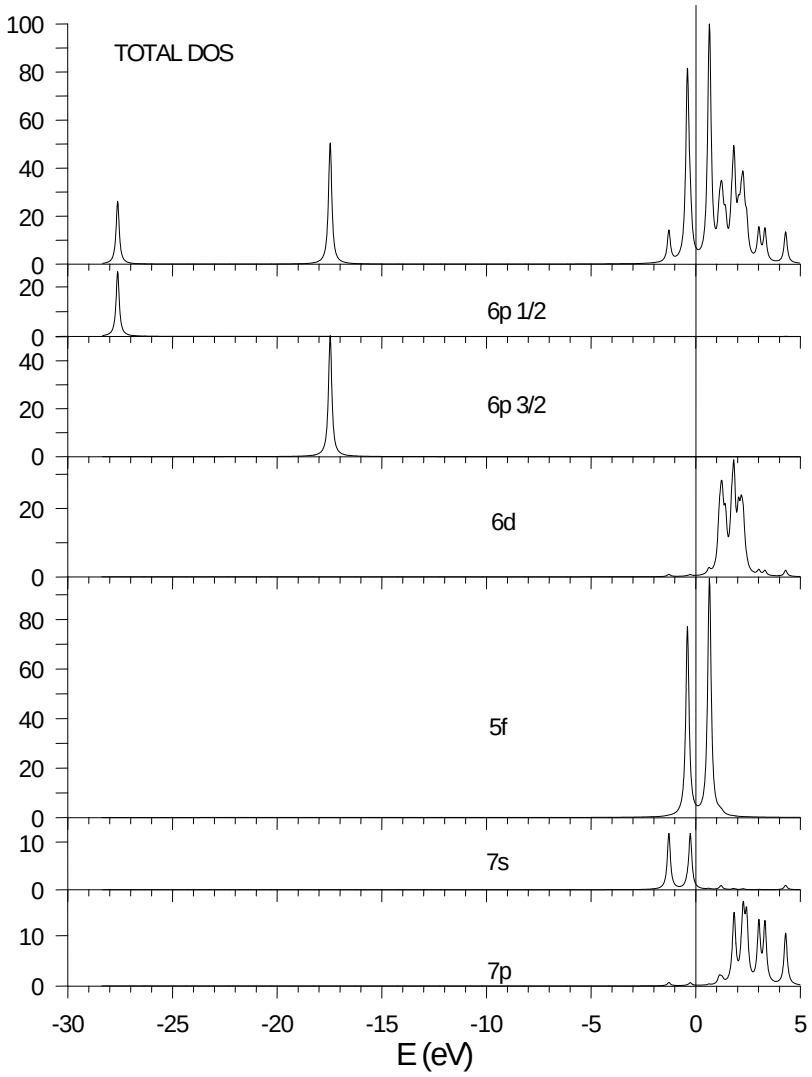

Figure I.2. Total and partial densities of states for the Pu_2 molecule with R_e = 4.5 Å.

results from different 5f contributions to these two MOs. The relativistic effects become considerable for deeper orbitals, e.g., the energy difference between Pu$6p_{1/2}$ and $6p_{3/2}$ is about 10.1 eV.

On the other hand, the considerable relativistic transformation of the core and semicore states could lead to the change in nucleus screening and, therefore, to the additional transformation of the structure of valence orbitals. In the case of An_2 these indirect relativistic effects can induce the change of the degree of 5f states delocalization. The latter effect could be evaluated by the values of overlap populations of various pairs of AOs of neighboring atoms (n_{ij}), which can also give the bond orders of these states [18]. Since in the $D_{\infty h}$ symmetry both An atoms are equivalent we reduced the symmetry of Pu_2 molecule to C_1 with two formally nonequivalent metal sites. Another problem of chemical bonding study concerns the influence of virtual 7p basis functions on the interactions of 5f, 6d, and 7s orbitals with each other. For this reason for Pu_2, Np_2 and Am_2 we performed two set of RDV calculations, one of them uses extended bases with 7p functions, while the second uses minimal bases without 7p AOs.

Table 2. Overlap populations of 6d, 5f, and 7s orbitals (in the units of 10^{-3} e) for Pu_2 with *minimal* bases and R_e = 4.5 Å. Total values for $d_{3/2}$ and $d_{5/2}$, $f_{5/2}$ and $f_{7/2}$ are given.

		Pu (2)		
		5f	6d	7s
Pu (1)	5f	1	4	1
	6d	4	27	27
	7s	1	27	-18

Table 3. Overlap populations of 6d, 5f, and 7s orbitals (in the units of 10^{-3} e) for Pu_2 with *extended* bases and R_e = 4.5 Å. Total values for $d_{3/2}$ and $d_{5/2}$, $f_{5/2}$ and $f_{7/2}$ are given.

		Pu (2)			
		5f	6d	7s	7p
Pu (1)	5f	1	4	1	1
	6d	4	25	27	10
	7s	1	27	-6	51
	7p	1	10	51	11

The values of n_{ij} for 6d, 5f, 7s, and 7p AOs of two plutonium atoms, which were obtained in our calculations for R_e = 4.5 Å are listed in Tables 2 and 3. Examination of Table 2 reveals that 6d and 7s orbitals play the main role in chemical bonding of dimer. The contribution of 5f AOs to bonding with 6d states is more than six times less than that of the main 6d-7s and 6d-6d

interactions. The overlap populations of 7p states shown in Table 3 change considerably the structure of bonding in Pu_2. The value of n_{ij} for 7p-7s is almost two times higher than that for 6d-7s AOs. A comparison of Table 2 and 3 shows that the inclusion of additional 7p basis functions also decreases the antibonding character of 6s-6s interaction in plutonium dimer. To determine the final valence orbital populations, the Mulliken population analysis was performed. It was found that plutonium atomic configuration in dimer can be described as $5f^{5.82}6d^{0.64}7s^{1.53}$ and $5f^{5.85}6d^{0.58}7s^{1.40}7p^{0.17}$ for two bases, respectively. Note that 7p AO population is the result of electron density shift mainly from 7s states, while the populations of 5f shell are nearly the same in both calculations.

Since different theoretical approaches give a quite considerable difference in equilibrium distances for Np_2 and Am_2, we performed, for both molecules, two sets of calculations with the "end" R_e values, i.e. 3.0 and 3.7 Å for Np_2, as well as 4.72 and 5.34 Å for Am_2. The values of n_{ij} for 6d, 5f, 7s, and 7p AOs of neptunium atoms we obtained in the calculations for R_e = 3.0 Å are listed in Tables 4 and 5. A comparison of the overlap populations in Tables 4, 5 with the results for Pu_2 shows that the 6d-6d interaction in neptunium dimer is stronger by the order of the magnitude. The contribution of Np5f AOs to bonding with 6d states is also considerably higher than that in Pu_2. The character of 7s-7s interaction changes from antibonding to strongly bonding when going from Pu_2 to Np_2. The overlap populations of 7p states shown in Table 5 are also essential but do not basically change the structure of bonding in Np_2. It was found that the

Table 4. Overlap populations of 6d, 5f, and 7s orbitals (in the units of 10^{-3} e) for Np_2 with *minimal* bases and R_e = 3.0 Å.

		Np (2)		
		5f	6d	7s
Np (1)	5f	15	45	0
	6d	45	235	29
	7s	0	29	57

Table 5. Overlap populations of 6d, 5f, 7s, and 7p orbitals (in the units of 10^{-3} e) for Np_2 with *extended* bases and R_e = 3.0 Å.

		Np (2)			
		5f	6d	7s	7p
Np (1)	5f	17	45	0	1
	6d	45	221	29	26
	7s	0	29	120	80
	7p	1	26	80	12

neptunium atomic configuration in dimer with R_e = 3.0 Å can be described as $5f^{4.09}6d^{1.72}7s^{1.21}$ and $5f^{4.10}6d^{1.64}7s^{1.05}7p^{0.21}$ for two bases respectively. The calculated overlap populations of neptunium atoms for R_e = 3.7 Å are listed in Tables 6 and 7. A comparison of n_{ij} values for two bond lengths shows that 6d-6d interaction for 3.7 Å is two times weaker than that for 3.0 Å. The contribution of 5f orbitals to bonding decreases even more. The character of 7s-7s interaction becomes antibonding as in Pu_2. The inclusion of 7p states in the basis changes the structure of bonding in a similar way as for shorter bond length. It was found that neptunium atomic configurations in dimer with R_e = 3.7 Å are $5f^{4.13}6d^{1.44}7s^{1.45}$ and $5f^{4.15}6d^{1.33}7s^{1.25}7p^{0.26}$. Note that the increase of R_e in Np_2 induces the shift of electron density from 6d to 7s states.

According to our calculations, Am_2 is the least bonded dimer in this series. The values of n_{ij} for valence AOs of americium atoms, which were calculated for R_e = 4.72 Å and 5.34 Å are listed in Tables 8, 9 and 10, 11, respectively. Examination of these four tables reveals that the interactions of all americium valence orbitals with each other at R_e = 4.72 Å are noticeably weaker than corresponding interactions in Pu_2 with similar bond length 4.5 Å. The contribution of americium orbitals to bonding at R_e = 5.34 Å is nearly two times less than corresponding values for 4.72 Å However, the atomic configurations predicted for 4.72 Å ($5f^{6.89}6d^{0.50}7s^{1.61}$ and $5f^{6.90}6d^{0.44}7s^{1.49}7p^{0.16}$) and for 5.34 Å ($5f^{6.90}6d^{0.45}7s^{1.65}$ and $5f^{6.91}6d^{0.40}7s^{1.56}7p^{0.13}$) are close to each other.

Table 6. Overlap populations of 6d, 5f, and 7s orbitals (in the units of 10^{-3} e) for Np_2 with *minimal* bases and R_e = 3.7 Å.

		Np (2)		
		5f	6d	7s
Np (1)	5f	3	15	0
	6d	15	124	39
	7s	0	39	-25

Table 7. Overlap populations of 6d, 5f, 7s, and 7p orbitals (in the units of 10^{-3} e) for Np_2 with *extended* bases and R_e = 3.7 Å.

		Np (2)			
		5f	6d	7s	7p
Np (1)	5f	3	15	0	1
	6d	15	114	38	26
	7s	0	38	24	88
	7p	1	26	88	15

Table 8. Overlap populations of 6d, 5f, and 7s orbitals (in the units of 10^{-3} e) for Am_2 with *minimal* bases and R_e = 4.72 Å.

		Am (2)		
		5f	6d	7s
Am (1)	5f	0	2	0
	6d	2	17	21
	7s	0	21	-19

Table 9. Overlap populations of 6d, 5f, 7s, and 7p orbitals (in the units of 10^{-3} e) for Am_2 with *extended* bases and R_e = 4.72 Å.

		Am (2)			
		5f	6d	7s	7p
Am (1)	5f	0	2	0	0
	6d	2	15	22	8
	7s	0	22	-9	43
	7p	0	8	43	11

Table 10. Overlap populations of 6d, 5f, and 7s orbitals (in the units of 10^{-3} e) for Am_2 with *minimal* bases and R_e = 5.34 Å.

		Am (2)		
		5f	6d	7s
Am (1)	5f	0	0	0
	6d	0	7	11
	7s	0	11	-9

Table 11. Overlap populations of 6d, 5f, 7s, and 7p orbitals (in the units of 10^{-3} e) for Am_2 with *extended* bases and R_e = 5.34 Å

		Am (2)			
		5f	6d	7s	7p
Am (1)	5f	0	0	0	0
	6d	0	7	11	5
	7s	0	11	-6	23
	7p	0	5	23	8

Since the equilibrium distance in molecular plutonium is considerably higher than that in any known actinide solid phase we also study the main features of chemical bonding transformation when Pu–Pu bond length decreases from 4.5 Å (isolated molecule) to 3.28 Å (δ-Pu) and 2.6 Å (α-Pu). Tables 12 and 13 list the values of overlap populations of valence MOs in Pu_2 obtained for R_e = 3.28 and 2.6 Å, respectively. Since the role of additional 7p basis functions is evident from the above results, the rest part of calculations was performed with the extended bases only. The comparison of Tables 3, 12, and 13 reveals that the contribution of all AOs to chemical bonding noticeably increases for the shorter bond lengths. Such a variation of n_{ij} is an expected result, however, for R_e = 2.6 Å the 6d-6d overlap population is only two times higher than for R_e = 3.28 Å, whereas the 5f-5f and 7s-7s overlaps increase by a factor of more than six and more than two, respectively. On the other hand, the examination of atomic configurations $5f^{5.80}6d^{0.98}7s^{1.04}7p^{0.18}$ (3.28 Å) and $5f^{5.77}6d^{1.26}7s^{0.89}7p^{0.09}$ (2.6 Å) reveals that 5f AOs population is the most stable with respect to the R_e variation as compared to the populations of 6d, 7s and 7p orbitals.

Table 12. Overlap populations of 6d, 5f, 7s, and 7p orbitals (in the units of 10^{-3} e) for Pu_2 with extended bases and R_e = 3.28 Å

		Pu (2)			
		5f	6d	7s	7p
Pu (1)	5f	12	32	0	0
	6d	32	121	38	16
	7s	0	38	78	80
	7p	0	16	80	11

Table 13. Overlap populations of 6d, 5f, 7s, and 7p orbitals (in the units of 10^{-3} e) for Pu_2 with extended bases and R_e = 2.6 Å

		Pu (2)			
		5f	6d	7s	7p
Pu (1)	5f	69	85	0	-3
	6d	85	203	9	-1
	7s	0	9	212	49
	7p	-3	-1	49	3

In summary, our theoretical investigations of actinide dimers confirm the earlier obtained results that such molecules can exist but with more long equilibrium interatomic distances than

in real solids. The examination of chemical bonding in Np_2, Pu_2 and Am_2 shows that the significant decrease of binding energies in the second (heavy) part of An_2 series is not simply due to the localization of 5f orbitals. According to our relativistic calculations the contribution of 5f AOs to bonding even in Np_2 (with quite high atomization energy and short bond length) is quite small as compared to the role of 6d, 7s and 7p states. However, the investigation of plutonium dimer with various equilibrium distances reveals that 5f-5f and 5f-6d interactions are extremely sensitive to the molecular size. The obtained populations of 5f shell in Np_2, Pu_2 and Am_2 are close to the formal configurations of isolated atoms, i.e. $5f^4$, $5f^6$ and $5f^7$, respectively.

I.3. Electronic structure calculations for Pu_{19}

The calculation of electronic structure of Pu_2 dimer with the bond length 3.28 Å corresponding to interatomic distances in δ-Pu could serve as a simple test of the transformation of Pu–Pu chemical bonding for R_e less than that of dimer. In the crystal lattice of fcc δ-Pu each metal site has twelve nearest neighbors and it is evident that the structure of chemical bonding for such a coordination differs essentially from that for a simple linear molecule. As a first step of investigation of chemical bonding and the role of 5f electrons in δ-Pu we consider the simple cluster model of this crystal consisting of only nineteen plutonium atoms. The structure of this cluster is illustrated in Fig. I.3 The electronic structure of Pu_{19} cluster was calculated using the RDV method with local exchange-correlation potential [19]. For the modeling of boundary conditions we used an “extended cluster” scheme described in details in Refs. [20,21]. In this model the crystal fragment under study consists of two parts: the internal main part (or the “core” of the cluster) and the outer part (or the “shell”). The outer part usually includes the atoms from 1 to 5 coordination spheres surrounding the “core”. During the self-consistency procedure the electron densities and the potential of the atoms in the “shell” are replaced by the corresponding values obtained for the crystallographically equivalent centers of the cluster “core”. Beside, to introduce the long-range component of the surrounding-crystal potential, the extended cluster is embedded into a pseudopotential formed by the outer crystal lattice which includes a few thousands of centers. Coulomb and exchange-correlation potentials of these pseudocenters are also substituted by the corresponding values obtained for the equivalent atoms in the internal part of the cluster [22].

Since in the present calculations we are interested in the interaction of the central atom with its nearest neighbors, the “core” of Pu_{19} cluster includes only one atom in the center of cluster (labeled below as Pu_1). Twelve plutonium sites of the next coordination sphere (Pu_2) and

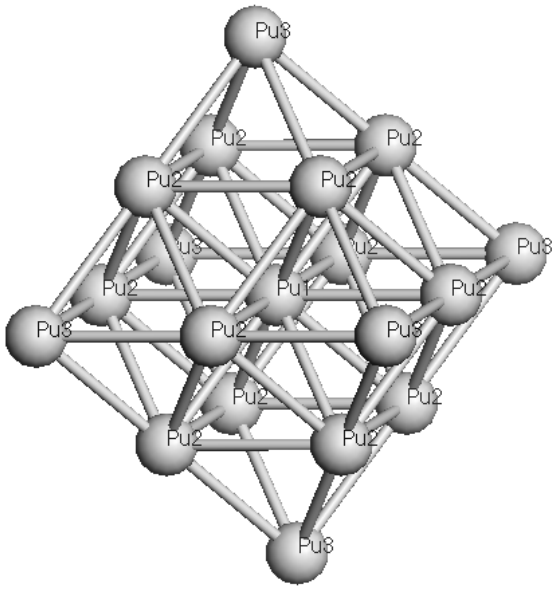

Figure I.3. The structure of Pu_{19} cluster of fcc Pu. Pu_1 is the central atom of the cluster, twelve Pu_2 atoms are its nearest neighbors, and six Pu_3 are the next nearest neighbors of the central atom.

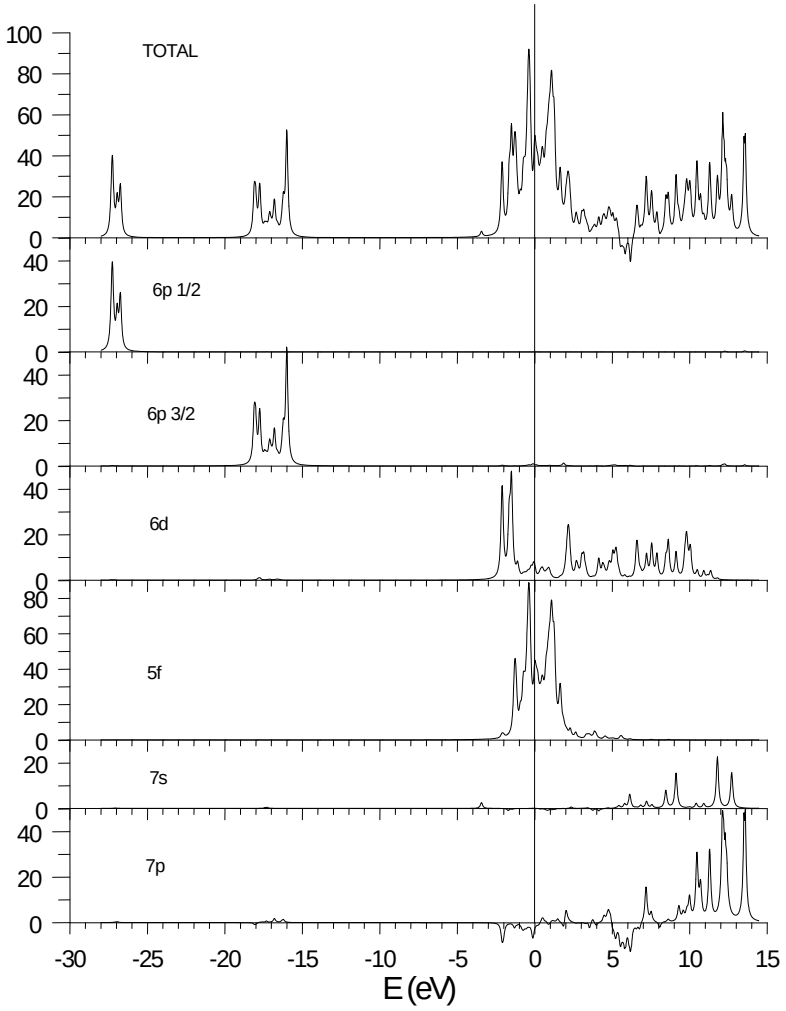

Figure I.4. Total and partial densities of states for the Pu_{19} cluster.

six next nearest neighbors (Pu_3) form the "shell" and during self-consistency their electron densities and potentials were kept equivalent to those of Pu_1. The extended bases of 4-component numerical atomic orbitals also included $7p_{1/2}$ and $7p_{3/2}$ functions. To ensure the convergence of valence MO energies within 0.1 eV, numerical Diophantine integration in matrix elements calculations was carried out for a set of 102000 points.

The total and partial densities of states obtained for the central Pu_1 atom in Pu_{19} cluster are shown in Fig. I.4. Since the partial DOS for $7p_{1/2}$ and $7p_{3/2}$, $6d_{3/2}$ and $6d_{5/2}$, $5f_{5/2}$ and $5f_{7/2}$ are close to each other, the sums of DOS for these MOs are presented in the figure. A comparison of DOS in figures I.2 and I.4 shows transformation of the discrete molecular levels (presented by sharp peaks in Fig. I.2) to real energy bands of various widths (Fig. I.4). For example, 76 MO levels of $6p_{3/2}$ type in Pu_{19} form energy band of the width about 2.5 eV. However, the spin-orbital splitting of $6p_{1/2}$ and $6p_{3/2}$ states is about 10 eV in both cases (for Pu_{19} this value was obtained for the centers of gravity of Pu$6p_{1/2}$ and $6p_{3/2}$ bands). Another important feature concerns the 6d band. As distinct from a molecule many states of this type turn out to be occupied in the Pu_{19} cluster (Fig. I.4). The electronic structure transformation, when going from a molecule to the cluster, is accompanied by considerable (nearly three times) increase of the width of vacant electronic states. Particularly, the highest 7p levels have the energy close to 14 eV. There is no energy gap in the Pu_{19} cluster, i.e. the energy difference of HOMO and LUMO is less than 0.01 eV. The HOMO in Pu_{19} contains 52% of 5f AOs of Pu_2 sites and 13% of Pu_3 5f states with admixtures of Pu_2 6d (19%) and Pu_3 6d (8%). There are no noticeable contributions to HOMO from any states of central Pu_1 atom. On the contrary, the LUMO contains 17% of Pu_1 5f AOs though the main contributions are also belong to Pu_2 5f (32%) and Pu_3 5f (23%) states.

Table 14. Overlap populations of 6d, 5f, and 7s orbitals (in the units of 10^{-3} e) for Pu_{19} with *minimal* bases per each $Pu_1 - Pu_2$ pair.

		Pu_2		
		5f	6d	7s
Pu_1	5f	8	18	0
	6d	19	75	13
	7s	0	9	24

Table 15. Overlap populations of 6d, 5f, 7s, and 7p orbitals (in the units of 10^{-3} e) for Pu_{19} cluster with *extended* bases per each $Pu_1 - Pu_2$ pair.

		Pu_2			
		5f	6d	7s	7p
Pu_1	5f	8	22	1	1
	6d	20	92	-2	23
	7s	0	1	8	-18
	7p	-5	-27	-48	-72

The values of overlap populations for 6d, 5f, 7s, and 7p AOs of Pu_1 and Pu_2 atoms obtained in the calculations of Pu_{19} cluster are listed in Tables 14 and 15. Note that in this case the matrixes of n_{ij} are not symmetrical due to non-equivalence of Pu_1 and Pu_2 sites in the cluster. Examination of Table 14 and 15 reveals that only 6d orbitals play the main role in chemical bonding of the cluster. The contributions of 7s-7s and 7s-6d AOs are noticeably less than corresponding values for dimer with the same Pu-Pu distance. Contribution of 5f electrons to bonding is also almost four times less than that of the main 6d-6d interaction. Note that this relation is nearly the same in Pu_2 and Pu_{19}. The overlap populations of 7p states shown in Table 15 are negative for almost all pairs of interacting orbitals. The antibonding role of 7p AOs is not too surprising result because the same effect was obtained for the (U,Pu)$7p_{3/2}$ – O2p interaction in oxides [23]. The Mulliken population analysis performed for Pu_{19} cluster gives the Pu_1 atomic configuration $5f^{5.15}6d^{2.55}7s^{0.40}$ and $5f^{5.48}6d^{3.22}7s^{0.08}7p^{-0.54}$ for two bases, respectively. The resulting population of virtual 7p AOs is negative due to the negative overlap of these functions belonging to nineteen atoms in the cluster. Note that the inclusion of 7p AOs in the bases considerably increases the population of 6d states, while the variation of N_f is relatively small.

I.4. Conclusions

Our investigations of a hypothetical plutonium dimer and 19-atom cluster corresponding to the fcc δ-Pu predict that the Pu5f states are noticeably hybridized with 6d orbitals of the nearest metal sites as well as with 5f AOs of the nearest neighbors in the molecule or in the crystal lattice. Due to this hybridization the number of 5f electrons could be quite different in simple dimer (N_f = 5.8) and in the system with high coordination of metal atom (N_f = 5.15 or 5.48). It is evident that small cluster Pu_{19} is too primitive model for the evaluation of metal –

metal interaction in δ-Pu. To obtain the more reliable results one needs to consider the clusters with considerably higher number of atoms.

References

1. J.G. Tobin et al., J. Phys.: Condens. Matter **20** (2008) 125204.
2. J.H. Shim et al., Nature **446** (2007) 513.
3. A. Mirmelstein et al., JETP Letters **90** (2009) 485.
4. K.A. Ginderich, Symp. Faraday Soc. **14** (1980) 109.
5. B.E. Bursten and G.A.Ozin, Inorg. Chem. **23** (1984) 2910; M. Pepper and B.E.Bursten, J. Am. Chem. Soc. **112** (1090) 7803; Chem. Rev. **91** (1991) 719.
6. E.F. Archibong and A.K. Ray, Phys. Rev.A. **60** (1999) 5105.
7. B. Delley, J. Chem. Phys. **92** (1990) 508; B. Delley, J. Chem. Phys. **113** (2000) 7756.
8. D.D. Koelling and B.N. Harmon, J. Phys. C: Solid State Phys. **10** (1977) 3107.
9. M. Douglas and N.M. Kroll, Acta Phys. **82** (1974) 89.
10. J.P. Perdew, K. Burke and M. Ernzerhof, Phys. Rev. Lett. **77** (1996) 3865.
11. A.D. Becke, J. Chem. Phys. **88** (1988) 2547; C. Lee, W. Yang and R.G.Parr, Phys. Rev.B. **37** (1988) 785.
12. J. Kubler and V. Eyert, Electronic Structure Calculations in Materials Science and Technology. Vol. 3A: Electronic and Magnetic Properties of Metals and Ceramics. Part I. Volume Ed.: K.H.J. Buschow (VCH-Verlag, Weinheim, 1992), p. 1-145.
13. A. Rosen and D.E. Ellis, J. Chem. Phys. **62** (1975) 3039.
14. H. Adachi, Technol. Reports Osaka Univ. **27** (1977) 569.
15. P. Pyykko and H. Toivonen, Acta Acad. Aboensis, Ser.B. **43** (1983) 1.
16. D.A. Varshalovich, A.N. Moskalev and V.K. Khersonskii, Quantum Theory of Angular Momentum (World Scientific, Singapore, 1988).
17. A. Rosen, Int. J. Quantum Chem. **XIII** (1978) 509.
18. R.S. Mulliken, Ann. Rev. Phys. Chem. **29** (1978) 1.
19. O. Gunnarsson, B.I. Lundqvist, Phys. Rev.B. **13** (1976) 4274.
20. M.V. Ryzhkov, N.I. Medvedeva, V.A. Gubanov, J. Phys. Chem. Solids **56** (1995) 1231.
21. M.V. Ryzhkov, T.A. Denisova, V.G. Zubkov, L.G. Maksimova, J. Struct. Chem. **41** (2000) 927.
22. D.E. Ellis, G.A. Benesh, E. Byrom, Phys. Rev.B. **20** (1979) 1198.
23. M.V. Ryzhkov, A.Ya. Kupryazhkin, J. Nuclear Materials. **384** (2009) 226.

Federal State Unitary Enterprise
"Russian Federal Nuclear Center – Zababakhin All-Russia Research Institute of Technical Physics"
FSUE "RFNC-VNIITF"

REPORT ON DETAILS OF THIRD AND FOURTH QUARTER RESULTS

Material Support Agreement No. B590089

"Electronic structure of Pu_{79} and Pu_{201} clusters. Training high-pressure X-ray diffraction experiments"

Snezhinsk 2011

Contents

Abstract

Fully relativistic *ab initio* discrete variational (RDV) method is used to calculate the structure of electronic states, chemical boding and electronic configurations of large Pu_{79} and Pu_{201} clusters being fragments of δ-Pu crystal lattice. Our results predict the vacant 6d states of an isolated atom to be populated in the fcc δ-Pu lattice as a result of significant redistribution of electron density from 5f and especially from 7s orbitals. Investigation of δ-Pu-like clusters formed by 79 and 201 atoms shows that plutonium 5f states are strongly hybridized with 6d orbitals of the nearest Pu sites. Due to this hybridization, the number of 5f electrons in an isolated atom ($N_f = 6$) and in the systems with high coordination numbers can be considerably different. The minimal value of $N_f = 4.9$ is obtained in the case of Pu_{201} cluster calculation with the minimal basis set (this is a preliminary result). The maximal value of $N_f = 5.5$ is obtained in the case of Pu79 cluster calculation with the extended basis that includes wave functions of virtual 7p states.

The analysis of chemical bonding in plutonium dimer, as well as in plutonium fcc clusters consisting of 19, 79, and 201 atoms, reveals that the main contributions to bonding are associated with the 6d-6d and 6d-5f interactions in all the cases under consideration and the relative structure of these contributions is similar in the systems of different sizes. Comparison of atomic configurations in plutonium dimer with bond length 3.28 Å and in fcc Pu_{19}, Pu_{79}, and Pu_{201} clusters with the same interatomic distance allows us to conclude that the decrease in N_f in clusters is due to high coordination number of plutonium atom in the fcc crystal.

A set of training X-ray diffraction experiments under high pressure was performed using STOE IPDS II diffraction system equipped with imaging plate detector and Almax-Boehler diamond anvil cell. In these experiments, we observed a structural phase transition in the $Ce_{0.9}Lu_{0.1}Ni$ compound and managed to detect anisotropy of α-uranium crystal lattice compression under quasi-hydrostatic external pressure.

I. Theoretical part. The RDV cluster calculations of the electronic configuration of face-centered cubic plutonium metal.

The general objective of the present work is quantum-chemical investigation of electronic structure and chemical bonding in plutonium metal using the cluster approach. These calculations can provide a more fundamental understanding of the plutonium atomic configuration transformation when going from an isolated atom to a molecular system and to a solid. Another goal of the work is independent evaluation of the number of 5f electrons in δ-Pu.

During the first half-year of the Contract implementation, we showed that significant decrease of binding energies in the heavy part of An_2 series is not simply due to the localization of 5f states, since the contribution of 5f atomic orbitals to the bonding even in Np_2 (with quite high atomization energy and short bond length) is quite small as compared to the role of 6d, 7s and 7p states. However, the investigation of plutonium dimer with various equilibrium distances reveals the 5f-5f and 5f-6d interactions to be extremely sensitive to the molecular size [1].

Besides, investigations of the plutonium dimer and 19-atom cluster corresponding to δ-Pu predicted noticeable hybridization of Pu 5f states with 6d orbitals of the nearest metal sites, as well as with 5f atomic orbitals of the nearest neighbors in the molecule or in the crystal lattice. Due to this hybridization, the number of 5f electrons could be quite different in the simple dimer (N_f = 5.8) and in the system with higher coordination of metal atom (N_f = 5.15 or 5.48) [1].

Relatively small Pu_{19} cluster is evidently a too primitive model for evaluation of "metal–metal" interaction in δ-Pu. To obtain the more reliable results, one needs to consider the clusters consisting of a much larger number of atoms. According to the Statement of Work, during the second half-year of the Contract the RDV calculations were performed for the electronic structure of large Pu_{79} and Pu_{201} clusters with fcc crystal-lattice boundary conditions.

To investigate the nature of chemical bonding and the role of 5f electrons in Pu_{79} and Pu_{201} clusters, we used the fully relativistic discrete variational method (RDV) [2,3]. The RDV method is based on the solution of the Dirac-Slater equation for the 4-component wave functions transforming according to the irreducible representations of the double point groups ($D_{\infty h}$ in the present calculations). To calculate the symmetry coefficients, we used the original code which realizes the projection operators technique [2] and includes the matrices of irreducible representations of double point groups obtained in Ref. [4], as well as the transformation matrices presented in Ref. [5]. The extended basis of the 4-component numerical atomic orbitals (AO) obtained as the solution of the Dirac-Slater equation for the isolated neutral atoms also included $An7p_{1/2}$ and $7p_{3/2}$ functions in addition to the occupied AOs.

I.1. Electronic structure of Pu_{79} cluster with fcc crystal-lattice boundary conditions (task I.3 of the Statement of Work)

The electronic structure calculations of Pu_2 dimer with the bond length 3.28 Å and of the small δ-Pu-like cluster Pu_{19} [1] can serve as a simple test of the Pu – Pu chemical bonding transformation due to the variation of coordination number. The next step to investigate the influence of crystal boundaries on the electron density redistribution shall be consideration of the greater size Pu_{79} and Pu_{201} clusters. In the fcc crystal lattice of δ-Pu, each metal site has twelve nearest neighbors and six next nearest neighbors. It is evident that the structure of chemical bonding for such a coordination number must be considerably different as compared to that of simple dimer. To model the boundary conditions, we used an "extended cluster" scheme described in details in Refs. [6,7]. In this model, the crystal fragment under study consists of two parts, i.e. the main internal part (the "core" of the cluster) and the outer part (the "shell"). The latter usually includes the atoms from 1 to 10 coordination spheres surrounding the "core". During the self-consistency procedure, the electron densities and the potential of the atoms in the "shell" are replaced by the appropriate values obtained for the crystallographically equivalent centers of the cluster "core". Besides, to introduce the long-range component of the surrounding-crystal potential, the extended cluster is embedded into a pseudopotential formed by the outer crystal lattice that includes a few thousands of centers. The Coulomb and exchange-correlation potentials of these pseudocenters are also substituted by the appropriate values obtained for the equivalent atoms in the internal part of the cluster [8].

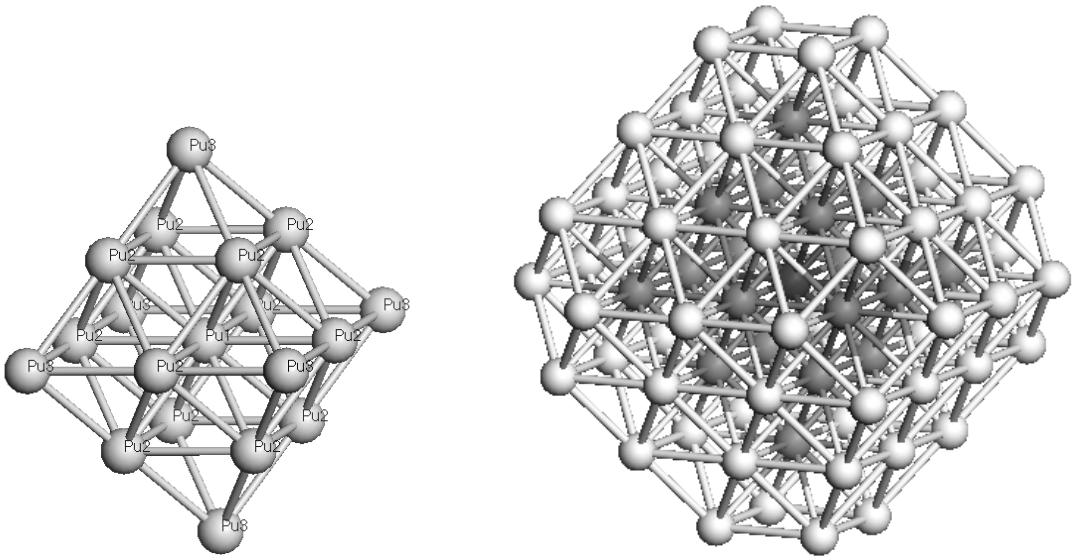

Figure I.1. The structure of δ-Pu-like Pu_{19} and Pu_{79} clusters. Pu_{79} cluster contains Pu_{19} as a "core" (showed as the dark spheres). Pu_1 is the central atom of Pu_{19} cluster, twelve Pu_2 and six Pu_3 atoms form its nearest neighbors and the next nearest neighbors, respectively.

The previously studied [1] simplest cluster model of δ-Pu contains only nineteen atoms, i.e. the central atom and its nearest and next nearest neighbors (Fig. I.1). The only "core" atom of Pu_{19} cluster is labeled as Pu_1. Twelve plutonium sites of the next coordination sphere (Pu_2) and six next nearest neighbors (Pu_3) form the "shell" and during self-consistency, their electron densities and potentials were kept equivalent to those of Pu_1. To ensure the convergence of valence MO energies within 0.1 eV, numerical Diophantine integration in matrix elements calculations was carried out for a set of 102000 points. Now this Pu_{19} cluster can serve as a "core" of the new fragment containing 79 atoms, i.e. Pu_{79} cluster (Fig. I.1). However, in this case there are no any restrictions with respect to the electronic characteristic of Pu_2 and Pu_3 centers during calculations. All three types of atoms in the "core" are considered simply as nonequivalent atoms in a molecule. The "shell" around the cluster "core" is formed by the atoms of the three next coordination spheres ($24Pu_4$, $12Pu_5$, and $24Pu_6$) providing the complete set of nearest neighbors for the atoms of a "core". During self-consistency, the electron densities and potentials of Pu_4, Pu_5, and Pu_6 were kept equivalent to those of Pu_1. To ensure the convergence of valence MO energies within 0.1 eV, numerical Diophantine integration in matrix elements calculations was carried out for 354000 sample points.

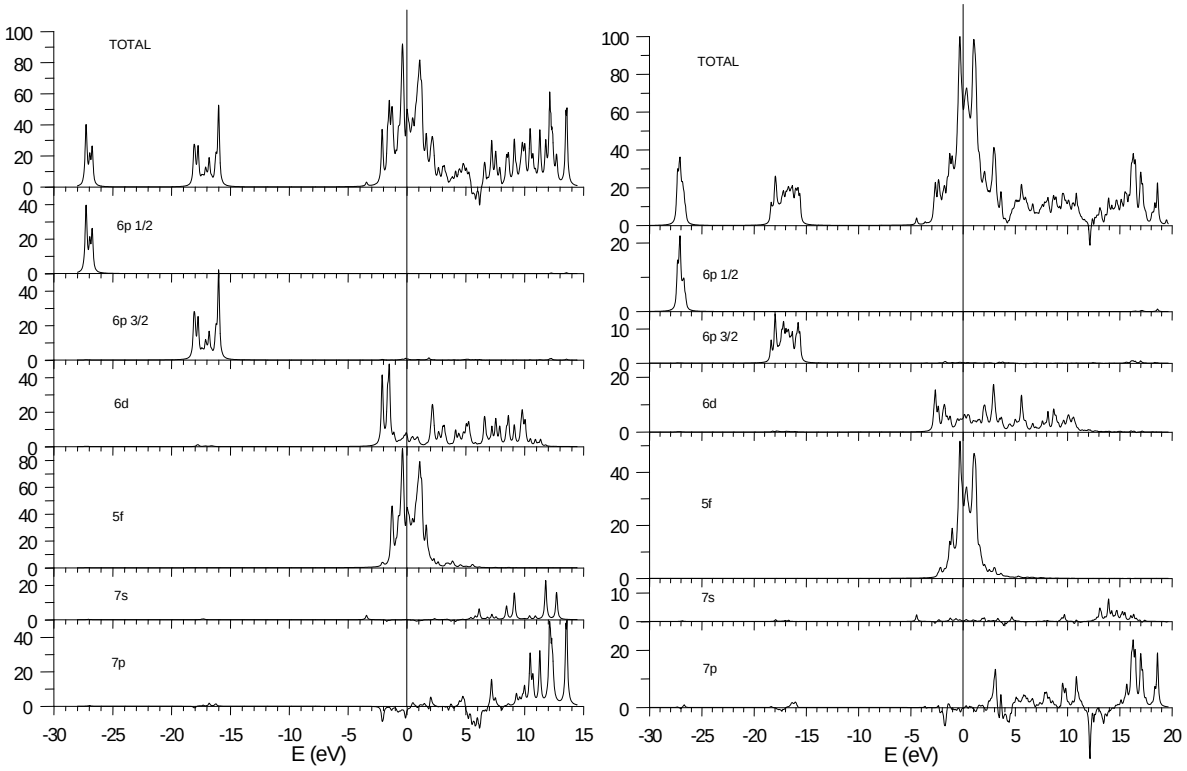

Pu_{19} **Pu_{79}**

Figure I.2. Total and partial densities of states for the central Pu_1 atom in Pu_{19} [1] and Pu_{79} clusters.

The total and partial densities of states (DOS) obtained for the central Pu_1 atom in Pu_{19} [1] and Pu_{79} clusters are shown in Fig. I 2. Since the partial DOS for $7p^{1/2}$ and $7p^{3/2}$, $6d^{3/2}$ and $6d^{5/2}$, $5f^{5/2}$ and $5f^{7/2}$ are close to each other, the sums of DOS for these MOs are presented in the figure. The comparison of results obtained for Pu_{19} and Pu_{79} shows that the positions and widths of the internal $6p_{1/2}$ and $6p_{3/2}$ bands are close in both cases, but the shapes of the bands are noticeably different. The line shape of external 6d states also transforms significantly. Besides, the left edge of this band shifts towards the lower energy (towards the higher binding energy), so that the energy difference between these edges in Pu_{79} and Pu_{19} clusters is 0.8 eV. At the same time, the upper edges of 6d bands in both cases lie at the same energy ~ 11 eV above the Fermi level (usually taken as zero of the energy scale). On the other hand, the positions and widths of 5f bands are close in both clusters. The only difference is found for their line shape. In both clusters, the occupied part of valence band is formed by the hybridized 5f – 6d orbitals, but the states at the bottom of this band are mainly of 6d character. The most pronounced difference is revealed for the delocalized 7s and 7p bands. The increase of cluster size leads to the increase of 7p AO contributions to the molecular states within the energy range between 0 and 5 eV above the Fermi level and to the considerable shift of the upper edge of 7s (from 13.5 eV in Pu_{19} to 17 eV in Pu_{79}) and 7p (from 14 eV in Pu_{19} to 19 eV in Pu_{79}) bands.

Similar to the case of Pu_{19} cluster [1], there is no energy gap in the Pu_{79} cluster, i.e. the energy difference between HOMO (the highest occupied molecular orbital) and LUMO (the lowest unoccupied molecular orbital) is less than 0.01 eV. HOMO in Pu_{79} contains only 3% of 5f AOs of Pu_1 site, 5% of 5f AOs of Pu_2, and 4% of Pu_3 5f states with admixtures of 3% of 6d AOs of these atoms, i.e. the main contributions to HOMO comes from the atoms of cluster “shell”, namely, 5f Pu_4 (29%), 5f Pu_5 (7%), and 5f Pu_6 (32%). In the small Pu_{19}, cluster there are no contributions to HOMO from any states of central Pu_1 atom. On the contrary, LUMO of Pu_{19} contains 17% of Pu_1 5f AOs while in LUMO of Pu_{79}, there are no contributions form the wave functions of central atom. The main contributions to LUMO of Pu_{79}, as well as to HOMO, belong to the Pu_2 5f (19%) and Pu_6 5f (35%) states.

Since the iteration process for Pu_{79} cluster involves two additional types of atoms, one can estimate the sensitivity of different cluster regions (types of atom) to the cluster boundary. In Fig. I.3, we compare the calculated DOS for Pu_1 and Pu_2 in Pu_{79} cluster. As seen, the positions and widths of most of the bands are close for both atom types, even the line shapes of 5f states are similar. Considerable transformation of DOS is observed for 7p orbitals. To apart from the pronounced qualitative difference in7p DOS intensity within the energy range between 0 and 10 eV, the DOS for Pu_1 contains noticeable negative contributions at the energies near 13 eV. This negative DOS results from the overlap of 7p wave functions of the central Pu_1 with orbitals of

the quite distant atoms in the crystal lattice. Such a difference in DOS of Pu_1 and Pu_2 is quite expectable since the actinide 7p orbitals are extremely delocalized and overlap with the electron density of atoms belonging to distant coordination spheres. The latter feature of these states makes the inclusion of 7p wave functions to the basis quite questionable. From the one hand, the extended basis set increases the variation freedom. From the other hand, calculations can give a negative value of occupation of this orbital, or the 7p occupation can accumulate the electron density belonging to other atoms. For this reason, the present stage of investigation, as in [1], also includes two types of calculations, i.e. with and without 7p basis functions.

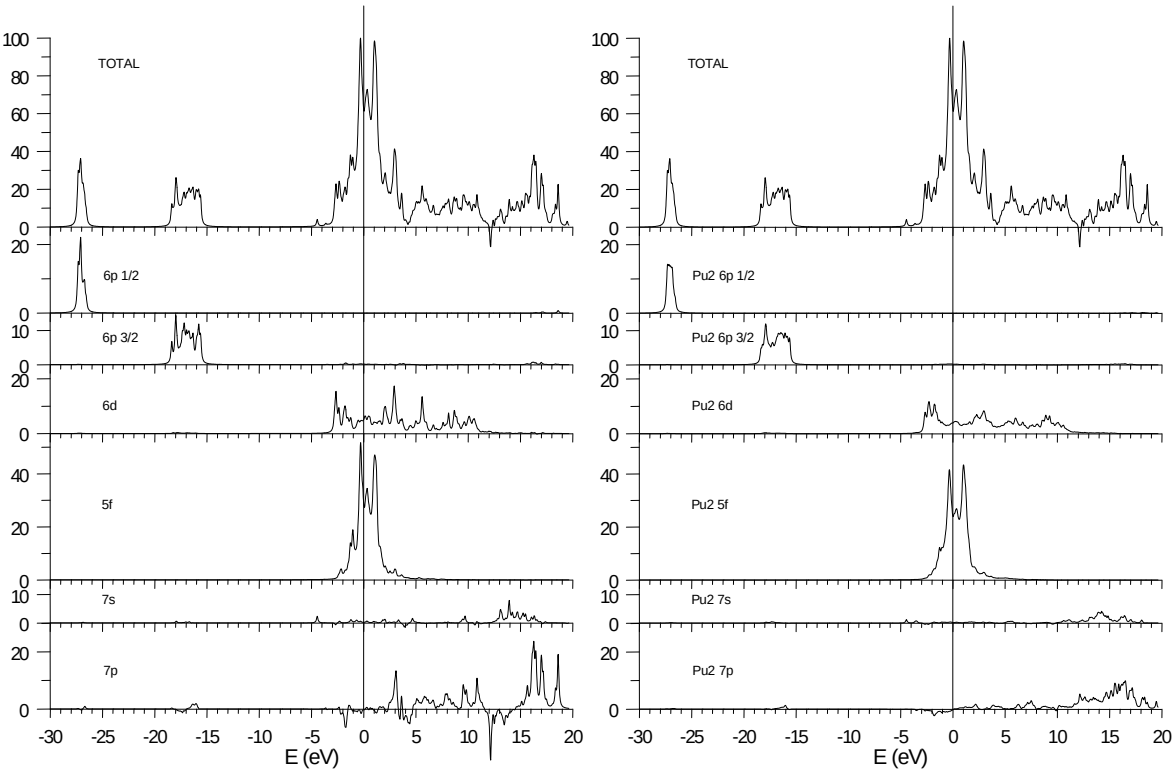

Pu_1 **Pu_2**

Figure I.3. Total and partial DOS for the central atom Pu_1 and for its nearest neighboring Pu_2 sites in Pu_{79} cluster.

The calculated values of overlap populations for 6d, 5f, 7s, and 7p AOs of Pu_1 and Pu_2 atoms in Pu_{19} [1] and Pu_{79} clusters are listed in Tables 1 and 2. Note that the matrixes of n_{ij} are not symmetrical due to non-equivalence of Pu_1 and Pu_2 sites in both clusters. Examination of Table 1 reveals that the contribution to bonding of 5f-5f, 5f-6d, and 6d-6d interactions remains almost unchanged with the cluster size increase. Only the small strengthening of 5f-5f and small weakening of 6d-6d bonds are observed. The main transformation is obtained for the 7s AOs contributions to bonding. The corresponding values in Pu_{79} cluster are considerably less than those in Pu_{19} cluster. Similar weakening of the bonding role of 7s states was obtained for the Pu_{19} cluster if the 7p functions were included into calculations [1]. The analysis of Table 2 shows

that the interactions between 5f and 6d states weakly depend on the cluster size. The 5f-5f bonding increases slightly in Pu_{79}, while the contribution of interactions of 7s AOs with 5f and 6d states to bonding becomes even weaker. The overlap populations of 7p states (Table 2) are negative for almost all pairs of interacting orbitals. The antibonding character of these orbitals increases with increasing cluster size. As previously mentioned [1], this is not something unexpected, because the same effect was observed for U-O2p and $Pu7p_{3/2}$ – O2p interactions in UO_2 and PuO_2 oxides [9].

Table 1. Overlap populations of 6d, 5f, and 7s orbitals (in the units of 10^{-3} e) for Pu_{19} [1] and Pu_{79} clusters with *minimal* basis per each Pu_1 – Pu_2 pair.

		Pu_{19}			Pu_{79}		
		Pu_2			Pu_2		
		5f	6d	7s	5f	6d	7s
Pu_1	5f	**8**	**18**	**0**	**11**	**16**	**0**
	6d	**19**	**75**	**13**	**19**	**70**	**1**
	7s	**0**	**9**	**24**	**1**	**-3**	**8**

Table 2. Overlap populations of 6d, 5f, 7s, and 7p orbitals (in the units of 10^{-3} e) for Pu_{19} [1] and Pu_{79} clusters with *extended* basis per each Pu_1 – Pu_2 pair.

		Pu_{19}				Pu_{79}			
		Pu_2				Pu_2			
		5f	6d	7s	7p	5f	6d	7s	7p
Pu_1	5f	**8**	**22**	**1**	**2**	**12**	**20**	**0**	**-2**
	6d	**20**	**92**	**-1**	**23**	**21**	**91**	**-6**	**26**
	7s	**0**	**3**	**26**	**-40**	**1**	**-1**	**22**	**-47**
	7p	**-5**	**-34**	**-56**	**-80**	**-6**	**-1**	**-112**	**-83**

The Mulliken population analysis performed for Pu_{79} cluster gives the atomic configurations $5f^{5.20}6d^{2.02}7s^{0.23}$ and $5f^{5.51}6d^{2.68}7s^{0.30}7p^{-0.24}$ of the central Pu_1 site for the minimal and extended basis, respectively (the corresponding values for Pu_{19} cluster are $5f^{5.15}6d^{2.55}7s^{0.40}$ and $5f^{5.48}6d^{3.22}7s^{0.08}7p^{-0.54}$ [1]). The resulting populations of virtual 7p AOs are always negative due to the negative overlap of these functions with the electron density of distant neighbors.

However, this effect decreases from $7p^{-0.54}(Pu_{19})$ [1] to $7p^{-0.24}(Pu_{79})$ with increasing cluster size. Note that the inclusion of 7p AOs to the basis strongly increases the population of 6d states (difference = 0.66), while the increase of 5f population (N_f) is two time less (difference = 0.31). Similar effect takes place in Pu_{19} cluster. Also, inclusion of the 7p functions causes weak increase of the 7s occupation in Pu_{79}, while in Pu_{19} cluster the 7s occupation significantly decreases.

The results of RDV calculations for Pu_{79} cluster allow us to estimate the effect of cluster boundary on the electronic configurations of a Pu ion. The configuration of the Pu_2 sites (the nearest neighbors of the central site) is found to be $5f^{5.38}6d^{2.65}7s^{0.38}$ (minimal basis) and $5f^{5.51}6d^{2.84}7s^{0.22}7p^{-0.27}$ (extended basis). From a comparison of electronic configurations of Pu_1 and Pu_2 sites in Pu_{79}, one can conclude that *i*) the boundary effect is more pronounced in the case of the minimal basis, and *ii*) the main difference is found for the population of 6d orbitals.

I.2. Electronic structure of Pu_{201} cluster with fcc crystal-lattice boundary conditions (continuation of task I.3 of the Statement of Work)

The next step of our investigation consists in the consideration of fcc Pu cluster formed by 201 atoms. The "core" of Pu_{201} cluster is the same as of Pu_{79}, i.e. Pu_{19} fragment formed by the central atom (Pu_1), its twelve nearest neighbors (Pu_2) and six next nearest neighbors (Pu_3). The "shell" surrounding cluster "core" contains atoms of the nine next coordination spheres ($24Pu_4$, $12Pu_5$, $24Pu_6$, $6Pu_7$, $48Pu_8$, $8Pu_9$, $12Pu_{10}$, $24Pu_{11}$, and $24Pu_{12}$). The distance from the end Pu_{12} atom to the center of Pu_{201} cluster is about 10.37 Å (the corresponding distance between Pu_6 and Pu_1 atoms in Pu_{79} cluster is about 7.33 Å). The structure of Pu_{201} cluster is illustrated in Fig. I.4. In this case during self-consistency the electron densities and potentials of the atoms from Pu_4 to Pu_{12} were kept equivalent to those of Pu_1. So, to ensure the convergence of valence MO energies within 0.1 eV, numerical Diophantine integration in matrix elements calculations was carried out for 842000 sample points.

The iteration process for such a big cluster is very time consuming. For this reason, the final self-consistency was not achieved by the mid April of 2011 (deadline for Report submission). Thus, this report includes the preliminary results of large cluster calculations. The final results will be presented later.

The total and partial densities of states obtained for the central Pu_1 atom in Pu_{79} and Pu_{201} clusters are shown in Fig. I.5. The comparison of DOS obtained for two large clusters shows that

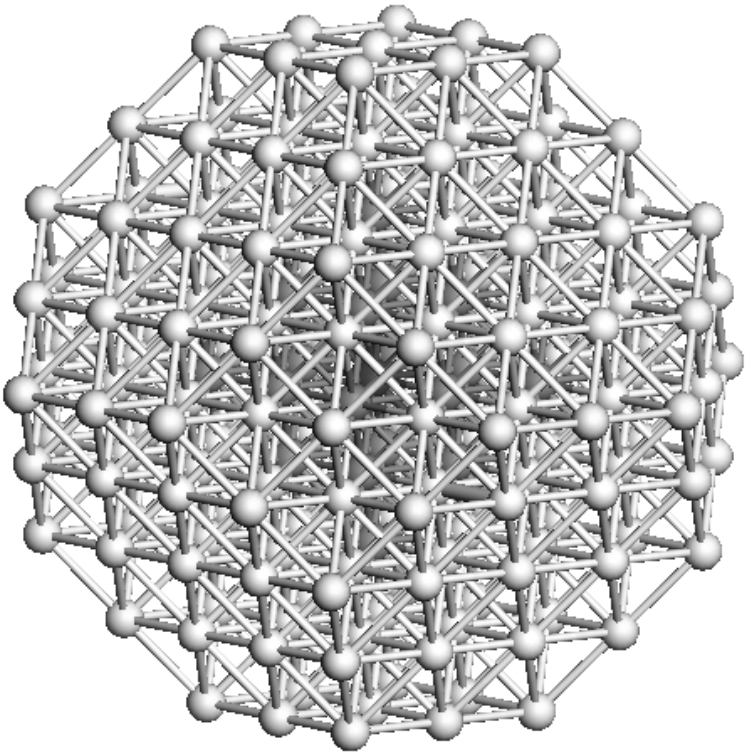

Figure I.4. The structure of δ-Pu-like Pu_{201}.

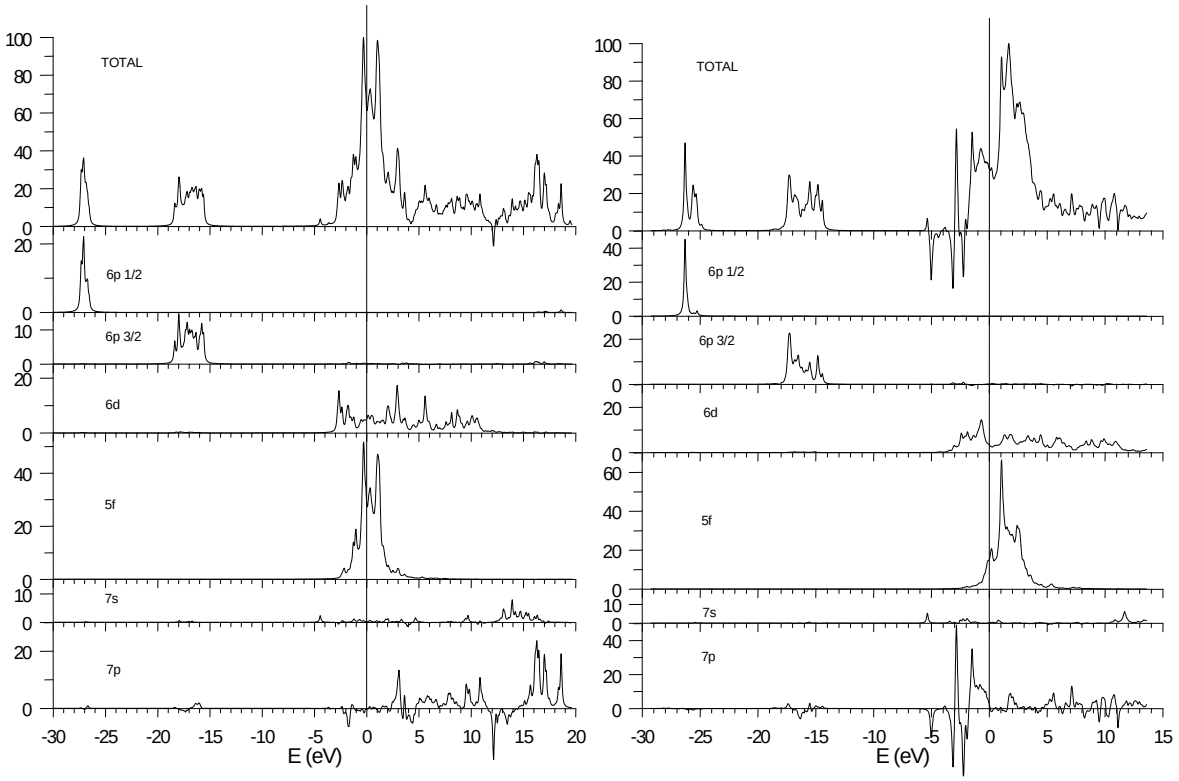

Pu_{79} **Pu_{201}**

Figure I.5. Total and partial densities of states for the central atom Pu_1 in Pu_{79} (the same as in the right panel of Fig.I.2) and Pu_{201} clusters.

the positions and widths of the internal $6p_{1/2}$ and $6p_{3/2}$ bands are close in both cases, but for the band shapes that differ. Besides the line shape transformation, significant shift (2 eV) towards the higher energy is found for the upper edge of external 6d states (as compared to the Pu_{79} cluster). The energies and widths of 5f bands are close in both clusters, the only difference is associated with their line shape. In the clusters of both sizes, the occupied part of valence band is formed by the hybridized 5f – 6d orbitals, but the bottom states of this band are mainly of the 6d character. The most significant difference is found for the delocalized 7p states. First, the increase of cluster size leads to the increase of the absolute value of 7p AOs contribution to the total DOS within the energy range between 0 and 5 eV below the Fermi level (both positive and negative significant contributions are presented). Second, admixture of these 7p AOs decreases essentially at the upper part of the vacant band above 10 eV. It should be emphasized that such a transformation of 7p band could be due to the incomplete self-consistency. Our experience suggests that 6d and 7s bands are getting stabilize first during the iteration procedure, then 5f states achieve their final parameters, and afterwards the final structure of 7p orbitals can be obtained.

Just as Pu_{19} and Pu_{79} clusters, Pu_{201} has no energy gap, difference between HOMO and LUMO is less than 0.01 eV. HOMO in Pu_{201} contains 20% of 5f AOs from Pu_8 sites, 14% of 5f AOs from Pu_{11}, and 34% of Pu_{12} 5f states with the 7% admixture of 6d AOs of the same atoms. In other words, the main contributions to HOMO (~75%) come from the atoms of the cluster "shell". In Pu_{201} cluster, there are no noticeable contributions to HOMO from any states of the central Pu_1 atom, as well as in Pu_{19} cluster. In the case of Pu_{201}, the contributions of the Pu_1 states are absent in LUMO as well. The LUMO of Pu_{201} contains 31% of Pu_8 5f AOs, 24% Pu_{12} 5f, and 11% of Pu_{11} 5f states.

Results obtained for the Pu_{201} cluster can be also used to estimate the sensitivity of various atom types to the cluster boundary. DOS for Pu_1 and Pu_2 for the Pu_{201} cluster are shown in Fig. 1.6. As seen, the positions and widths of almost all bands are similar for both types of atoms. The three-peak line shape of 5f states is found both for Pu_1 and Pu_2 sites, however the relative intensities of these peaks turn out to be different. Also, DOS of 7p orbitals transforms significantly within the energy range between 0 and 5 eV below the Fermi level when going from the central Pu_1 site to its nearest neighboring Pu_2. This behavior can be the result either of a delocalized character of 7p states or incomplete self-consistent procedure.

The calculated values of overlap populations for 6d, 5f, 7s, and 7p AOs of Pu_1 and Pu_2 atoms in Pu_{79} and Pu_{201} clusters are listed in Tables 3 and 4. From Table 3 it follows that the contribution to bonding of 5f-5f, 5f-6d, and 6d-6d interactions remains almost unchanged with the increase of cluster size. Some transformation is observed the 7s states. In Pu_{201} cluster, the

contribution of these states to bonding increases as compared to that in Pu_{79} cluster. Table 4 shows also that the interactions between 5f and 6d states are close in both clusters. In contrast to

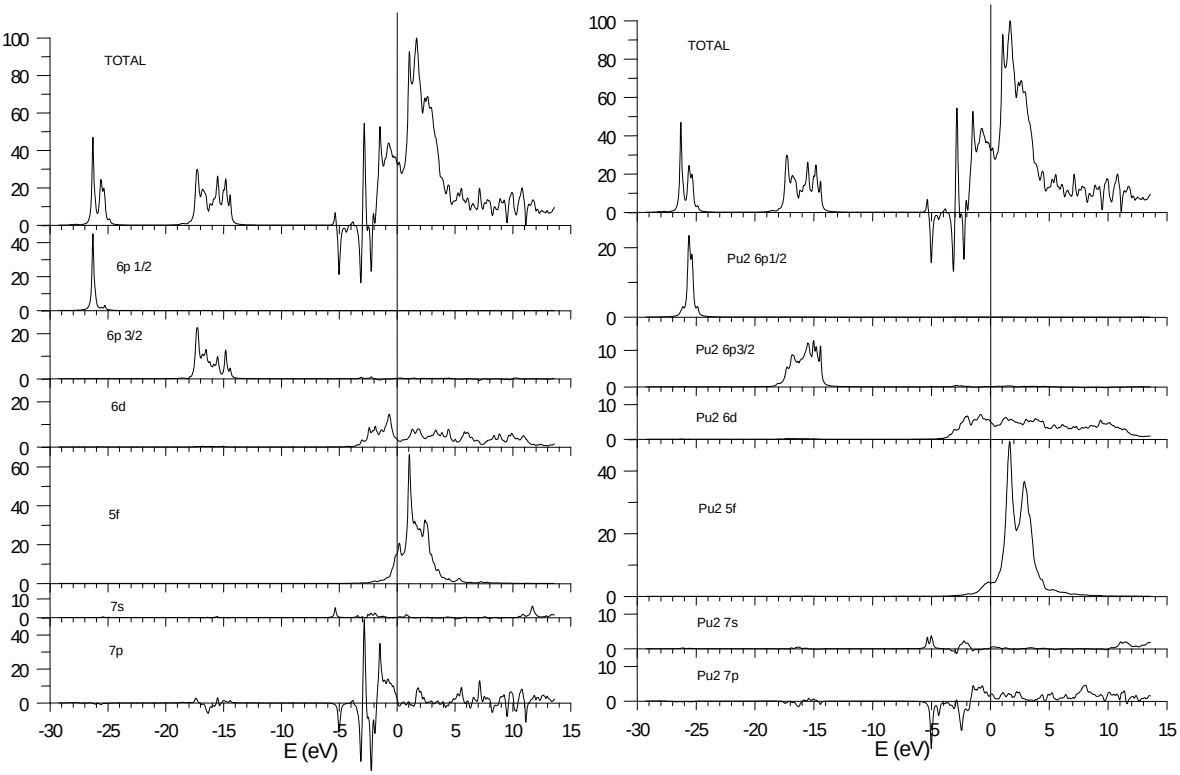

Pu_1 **Pu_2**

Figure I.6. Total and partial densities of states for the central Pu_1 atom and for its nearest neighboring Pu_2 sites in Pu_{201} cluster.

the n_{ij} transformation when the cluster size increases from 19 to 79 atoms (see section 1.2), there is no further weakening of the 7s AOs interaction with 5f and 6d states in 201-atoms cluster. The overlap populations of 7p states are negative for almost all pairs of interacting orbitals (Table 4). Antibonding character of these orbitals undergoes further increase with the cluster growth. Huge negative values of overlap populations for 7p-7p and 7s-7p AOs are most likely the result of incomplete iteration process.

The Mulliken population analysis performed for Pu_{201} cluster gives the Pu_1 electronic configurations $5f^{4.92}6d^{3.60}7s^{0.47}$ and $5f^{5.17}6d^{3.79}7s^{0.45}7p^{0.58}$ for the minimal and extended basis, respectively. The population of virtual 7p AOs, which is negative in two smaller clusters ($7p^{-0.54}$ in Pu_{19} and $7p^{-0.24}$ in Pu_{79}), becomes positive in the fcc crystal lattice fragment formed by 201 atoms. However, this is true for the central Pu_1 atom only, while calculations give the configuration $7p^{-0.35}$ for its nearest neighboring Pu_2 sites (see below). Again, it is quite possible that the positive population of Pu_1 7p AOs is due to incomplete self-consistent process. Note that, in contrast to the cases of smaller clusters, difference in the population of 6d states calculated with the minimal and extended basis is not so large. At the same time, the difference (equals 0.25) in 5f-state occupation (N_f) is close to the previous case. The occupation of 7s states

in Pu_{201} cluster is almost independent on the choice of the basis while this value is found to decrease strongly in the case with Pu_{19} cluster and slightly increase in the case with Pu_{79}.

Table 3. Overlap populations of 6d, 5f, and 7s orbitals (in the units of 10^{-3} e) for Pu_{79} and Pu_{201} clusters with minimal basis per each pair $Pu_1 – Pu_2$.

		Pu_{79}			Pu_{201}		
		Pu_2			Pu_2		
		5f	6d	7s	5f	6d	7s
Pu_1	5f	**11**	**16**	**0**	**12**	**23**	**1**
	6d	**19**	**70**	**1**	**23**	**92**	**-1**
	7s	**1**	**-3**	**8**	**1**	**-1**	**15**

Table 4. Overlap populations of 6d, 5f, 7s, and 7p orbitals (in the units of 10^{-3} e) for Pu_{79} and Pu_{201} clusters with extended basis per each pair $Pu_1 – Pu_2$.

		Pu_{79}				Pu_{201}			
		Pu_2				Pu_2			
		5f	6d	7s	7p	5f	6d	7s	7p
Pu_1	5f	**12**	**20**	**0**	**-2**	**14**	**17**	**0**	**-1**
	6d	**21**	**91**	**-6**	**26**	**25**	**111**	**1**	**74**
	7s	**1**	**-1**	**22**	**-47**	**0**	**0**	**43**	**-130**
	7p	**-6**	**-1**	**-112**	**-83**	**0**	**35**	**-451**	**-160**

Our calculations give $5f^{5.11}6d^{3.95}7s^{0.47}$ (minimal basis) and $5f^{5.41}6d^{3.83}7s^{0.47}7p^{-0.35}$ (extended basis) configurations for the nearest neighboring Pu_2 sites in Pu_{201} cluster. The main difference between Pu_1 and Pu_2 consists in the population of 5f and, at minimal basis, of 6d orbitals (excluding 7p states).

Table 5 and Fig. 1.7 summarize the RDV calculation results of the Pu electronic configuration for all the systems (dimer and Pu clusters formed by 19, 79, and 201 atoms) studied in the present Contract. One can see that occupation of 5f states displays a tendency to decrease with the increasing molecule size. On the contrary, occupations of the 6d and 7s states tend to increase. The 6d AOs occupation is the most sensitive to the choice of basis (minimal or extended), to the cluster size, as well as to the boundary effect. The latter follows from a

comparison of the occupation numbers for the central Pu_1 and nearest neighboring Pu_2 sites. As expected, the boundary effect decreases with the cluster size increase.

Table 5. The RDV results for electronic configurations of plutonium dimer Pu_2 and plutonium clusters formed by 19, 79, and 201 atoms. Dimer size as well as the nearest interatomc distance (bond length) in fcc clusters R = 3.28 Å corresponds to the crystal lattice parameter a = 4.638 Å of δ-Pu [10].

	basis	Pu_1 site	Pu_2 site
Pu_2 dimer (R = 3.28 Å)	minimal		
	extended	$5f^{5.80}6d^{0.98}7s^{1.04}7p^{0.18}$	
Pu_{19} cluster	minimal	$5f^{5.15}6d^{2.55}7s^{0.40}$	
	extended	$5f^{5.48}6d^{3.22}7s^{0.08}7p^{-0.54}$	
Pu_{79} cluster	minimal	$5f^{5.20}6d^{2.02}7s^{0.23}$	$5f^{5.38}6d^{2.65}7s^{0.38}$
	extended	$5f^{5.51}6d^{2.68}7s^{0.30}7p^{-0.24}$	$5f^{5.51}6d^{2.84}7s^{0.22}7p^{-0.27}$
Pu_{201} cluster	minimal	$5f^{4.92}6d^{3.60}7s^{0.47}$	$5f^{5.11}6d^{3.95}7s^{0.47}$
	extended	$5f^{5.17}6d^{3.79}7s^{0.45}7p^{0.58}$	$5f^{5.41}6d^{3.83}7s^{0.47}7p^{-0.35}$

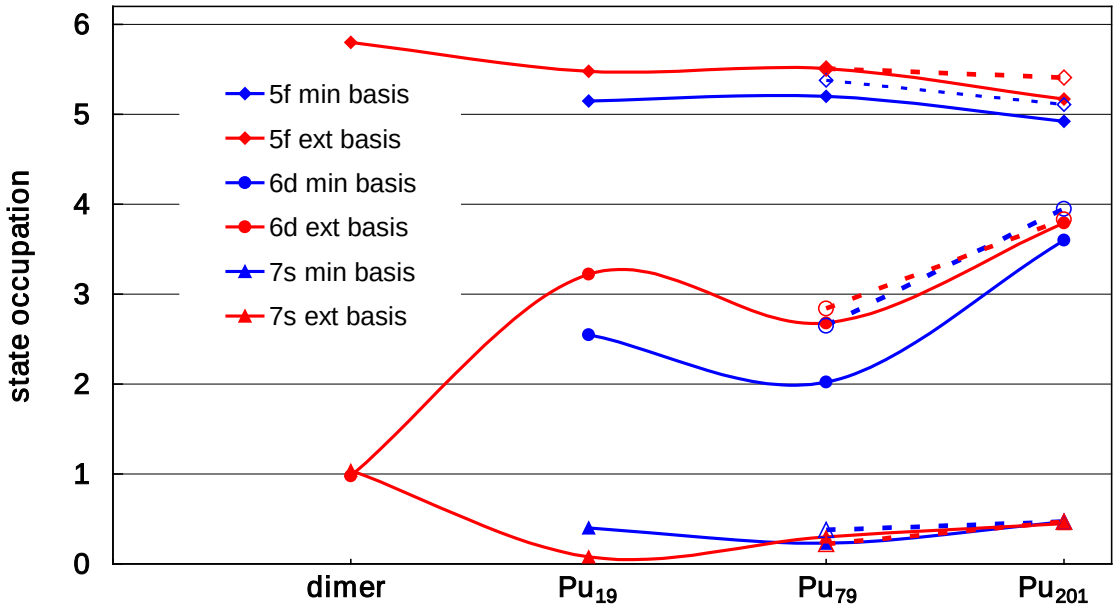

Figure I.7. Variation in the occupation of 5f, 6d, and 7s states of the central Pu_1 site vs. size of Pu cluster. Open signs and dasheds lines show the occupation of the same states for the nearest neighboring Pu_2 positions. The data from Table 5 are plotted.

I.3. Conclusions

The results obtained during the second half-year of the present Contract can be summarized as follows.

1. For the first time, the structure of electronic states and chemical bonding of large Pu_{79} and Pu_{201} clusters are obtained using the fully relativistic ab initio method.
2. Our investigations of the δ-Pu-like fcc clusters formed by 79 and 201 atoms predict strong hybridization of the plutonium 5f states with 6d and 5f atomic orbitals of the neighboring sites in the crystal lattice. Due to this hybridization, the number of 5f electrons in an isolated atom (N_f = 6) and in the systems with high coordination numbers could be considerably different. The lowest value of N_f = 4.9 is obtained from the calculations for the biggest Pu_{201} cluster with the minimal basis set, while the highest value N_f = 5.5 is found for the Pu_{79} cluster calculations with the extended basis which includes wave functions of virtual 7p states.
3. Our calculations show that the occupation of vacant 6d states in the δ-Pu crystal lattice results from significant redistribution of the electron density from 5f and especially from 7s orbitals.

References

1. "Electronic structure of actinide dimmers and Pu_{19} cluster. Training high-pressure X-ray diffraction experiments", Report on details of first and second quarter results, MSA No. B590089, Snezhinsk, 2011.
2. A. Rosen and D.E. Ellis, J. Chem. Phys. **62** (1975) 3039.
3. H. Adachi, Technol. Reports Osaka Univ. **27** (1977) 569.
4. P. Pyykko and H. Toivonen, Acta Acad. Aboensis, Ser.B. **43** (1983) 1.
5. D.A. Varshalovich, A.N. Moskalev and V.K. Khersonskii, Quantum Theory of Angular Momentum (World Scientific, Singapore, 1988).
6. M.V. Ryzhkov, N.I. Medvedeva, V.A. Gubanov, J. Phys. Chem. Solids, **56** (1995) 1231.
7. M.V. Ryzhkov, T.A. Denisova, V.G. Zubkov, L.G. Maksimova, J. Struct. Chem. **41** (2000) 927.
8. D.E. Ellis, G.A. Benesh, E. Byrom, Phys. Rev.B. **20** (1979) 1198.
9. M.V. Ryzhkov, A.Ya. Kupryazhkin, J. Nuclear Materials. **384** (2009) 226.
10. A.C. Lawson, J.A. Roberts, B. Martinez, M. Ramos, G. Kotliar, F.W. Trou, M.R. Fitzsimmons, M.P. Hehlen, J.C. Lashley, H. Ledbetter, R.J. MqQueeney, A. Migliory, Phyl Mag. **86** (2006) 2713.

Journal of Nuclear Materials 384 (2009) 226–230

Contents lists available at ScienceDirect

Journal of Nuclear Materials

journal homepage: www.elsevier.com/locate/jnucmat

First-principles study of electronic structure and insulating properties of uranium and plutonium dioxides

M.V. Ryzhkov [a,*], A.Ya. Kupryazhkin [b]

[a] Institute of Solid State Chemistry, Ural Branch of the Russian Academy of Sciences, Pervomaiskaya Str. 91, Ekaterinburg 620219, Russia
[b] Ural State Technical University, Mira Str. 19, Ekaterinburg 620219, Russia

ARTICLE INFO

Article history:
Received 25 March 2008
Accepted 18 November 2008

ABSTRACT

First-principles density functional theory calculations were carried out to investigate the electronic structure and the degree of 5f states localization of the Mott–Hubbard type insulators UO_2 and PuO_2. We used the fully relativistic cluster discrete variational method (RDV) with the local exchange-correlation potential. The energies of one-electron transition between occupied and vacant $5f^{5/2}$ states of neighboring actinide atoms were evaluated on the base of the ground state and the excited state calculations. It is found that in UO_2 and PuO_2 the energy difference between $5f^{5/2}$ levels of nearest metal sites in the lattice are close to 1.0 eV and 0.9 eV, despite the results of conventional band structure approach predicting that both oxides are good conductors.

1. Introduction

Though the electronic structure of the uranium and plutonium dioxides has been the subject of theoretical investigations over the last 30 years [1–6], some questions concerning the inclusion of all relativistic effects and correct description of their insulating properties are still unclear. It is known from experiments [7,8] that UO_2 and PuO_2 are the so-called Mott–Hubbard insulators, i.e. the occupied and vacant 5f bands are separated by the band gaps of 2.1 eV [7] and 1.8 eV [8] in UO_2 and PuO_2, respectively. However, when the electronic structure of UO_2 and PuO_2 is calculated using conventional first-principles methods such as the local density approximation (LDA) or generalized gradient approximation (GGA) these band gaps are not reproduced. Both the LDA and the GGA predict UO_2 and PuO_2 in the ground states to be good conductors. We know two approaches based on periodic boundary conditions, which appear to remedy the band gap problem. (1) The LDA + *U* model [9] of treating the strong correlation effects, in this method the orbital potential splits the 5f band of UO_2 into narrow occupied and broad unoccupied bands [4,5]. (2) The use of hybrid functionals for the exchange-correlation potential also predicts a non-zero band gap for uranium and plutonium oxides [6].

On the other hand, the crystallographically equivalent atomic sites become non-equivalent in the finite fragments of the lattice which are described with the use of point symmetry instead of translational symmetry in the band structure approach. Specifically, in the cluster models the absence of the band gap does not directly mean the metal conductivity because the highest occupied (HOMO) and the lowest unoccupied (LUMO) molecular orbitals could be located on the same atom. On the other hand, the energies of the occupied and vacant orbitals belonging to the nearest atomic sites could be noticeably different as in the case of semiconductors or even insulators. Furthermore, the electron transition between two atoms in the lattice could lead to the redistribution of charge density of several nearest sites and, therefore, to the additional shifts of the initial and final energy levels.

The aim of the present paper is the investigations of the properties of occupied and vacant 5f states of UO_2 and PuO_2 in the direct space approach. In this work we concentrate on a one-electron transition from the occupied to the vacant $5f^{5/2}$ molecular orbitals (MO) located on the neighboring actinide atoms. Our purpose is to evaluate the energy difference between initial and final levels of this transition in the ground state and in the excited state of these compounds.

2. Objects and methods of calculations

The ground state calculations of the electronic structure of UO_2 and PuO_2 were made for the 279-atom clusters $U_{63}O_{216}$ and $Pu_{63}O_{216}$ representing the fragments of dioxide lattices. The structure of these clusters is illustrated in Fig. 1. For the modeling of boundary conditions we used an "extended cluster" scheme described in details in Refs. [10,11]. In this model the crystal fragment under study consists of two parts: the internal main part (or the "core" of the cluster) and the outer part (or the "shell"), the latter part usually includes the atoms of 1–5 coordination spheres surrounding the "core". During the self-consistency procedure the electron densities and the potential of the ions in the "shell" are replaced by the corresponding values obtained for the

* Corresponding author. Tel.: +7 343 3623554; fax: +7 343 3744495.
E-mail address: ryz@ihim.uran.ru (M.V. Ryzhkov).

0022-3115/$ - see front matter © 2008 Elsevier B.V. All rights reserved.
doi:10.1016/j.jnucmat.2008.11.011

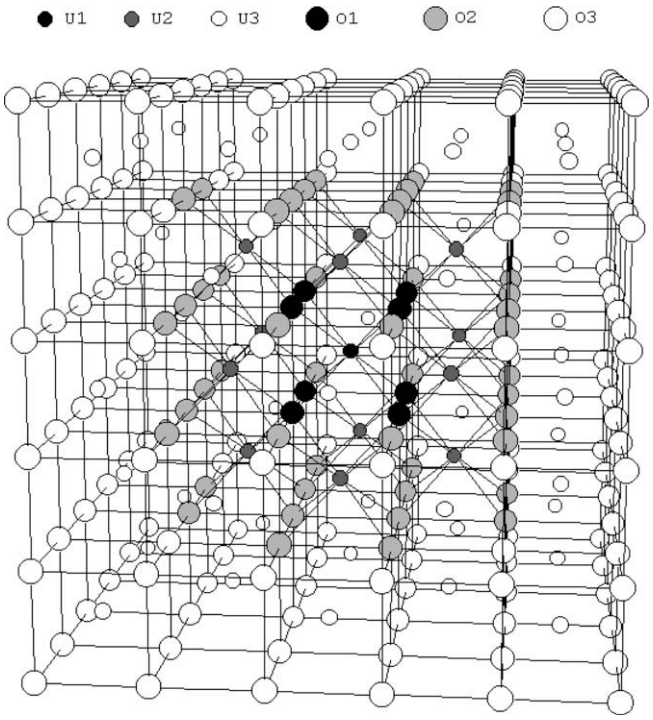

Fig. 1. The structure of $U(Pu)_{63}O_{216}$ cluster in the actinide dioxide lattice.

crystallographically equivalent centers of the cluster "core". In addition to introduce the long-range component of the surrounding crystal potential, the extended cluster is embedded in a pseudo-potential of the outer crystal lattice including 7972 centers with coulomb and exchange-correlation potentials obtained for the corresponding equivalent atoms in the internal part of the cluster [12].

In the present calculations the "core" of $Ac_{63}O_{216}$ clusters included: U(Pu) atom in the center with its eight nearest oxygen neighbors (these atoms are labeled below as U_1, Pu_1, O_1), 12 actinide sites of the next metal coordination sphere (U_2, Pu_2) with their 48 nearest ligands (O_2) forming two crystallographically non-equivalent groups (Fig. 1). The other atoms of the cluster (U_3, Pu_3, O_3) formed the "shell" and during self-consistency their electron densities and potentials were kept equivalent to those of $U_1(Pu_1)$ and O_1.

The investigation of the excited state corresponding to the electron transition between $5f^{5/2}$ molecular orbitals was performed using the Slater's "transition state procedure" [13]. In this method the population of initial occupied MO is decreased and the population of final vacant MO is increased by 0.5. The energy difference of these partially occupied levels obtained in the SCF calculation can serve as a measure of the relaxation effects which take place when 5f electron moves from one atom to another.

Since the transition state calculations for the 279-atomic clusters could not be done during reasonable time, we consider the quite small $Ac_{13}O_{56}$ clusters (the main part of $Ac_{63}O_{216}$) where 48 outer ligands (O_2) now form the "shell" around AcO_8Ac_{12} "core" and during self-consistency their density and potential were kept equivalent to those of O_1. The rest sites of $Ac_{63}O_{216}$ fragment were added to the pseudo-potential part of the boundary condition of $Ac_{13}O_{56}$. Another problem of excited state calculations concerns the fact that the transition of an electron from one individual atom (U_1 or Pu_1) to the individual atom of the next coordination sphere of Ac breaks the equivalency of $12U_2(Pu_2)$ sites. For this reason we changed the orientation of coordinate axes and reduced the symmetry of $Ac_{13}O_{56}$ clusters from D_{4h} to C_{2v}.

In this work the electronic structure was calculated in the density functional theory approximation (DFT) using the original code of the fully relativistic discrete variational cluster method (RDV) [14,15] with local exchange-correlation potential [16]. The RDV method is based on the solution of the Dirac–Slater equation for 4-component wave functions transforming according to irreducible representations of the double point groups (in the present calculations – D_{4h} and C_{2v}). For the calculation of symmetry coefficients we used the original code which realizes the projection operators technique [14] and includes the matrices of irreducible representations of double point groups obtained in Ref. [17] and the transformation matrices presented in Ref. [18]. The extended bases of 4-component numerical atomic orbitals (AO) obtained as the solution of the Dirac–Slater equation for the isolated neutral atoms also included $Ac7p^{1/2}$ and $7p^{3/2}$ functions in addition to occupied AOs. Numerical diophantine integration in matrix elements calculations was carried out for 700 000 ($Ac_{63}O_{216}$) and 178 000 ($Ac_{13}O_{56}$) sample points, that provided the convergence of valence MO energies within 0.1 eV. The effective charges on atoms (Q_{eff}) were computed as the integrals of electron density inside the domains bounded by the points of its minimum [19].

3. Results and discussion

The total and partial densities of states (DOS) obtained for the central $U_1(Pu_1)$ and O_1 atoms in $Ac_{63}O_{216}$ clusters are shown in Figs. 2 and 3. Since the partial DOS for $Ac7p^{1/2}$ and $7p^{3/2}$, $Ac6d^{3/2}$ and $6d^{5/2}$, $O2p^{1/2}$ and $O2p^{3/2}$ are close to each other, the sum of DOS for 7p, 6d and O2p MOs are presented in the figures. The comparison of our results with those obtained in conventional band structure calculations of UO_2 and PuO_2 [2,6] shows that the structure of valence and vacant states of the central part of $Ac_{63}O_{216}$ clusters are close to the positions and widths of the valence and

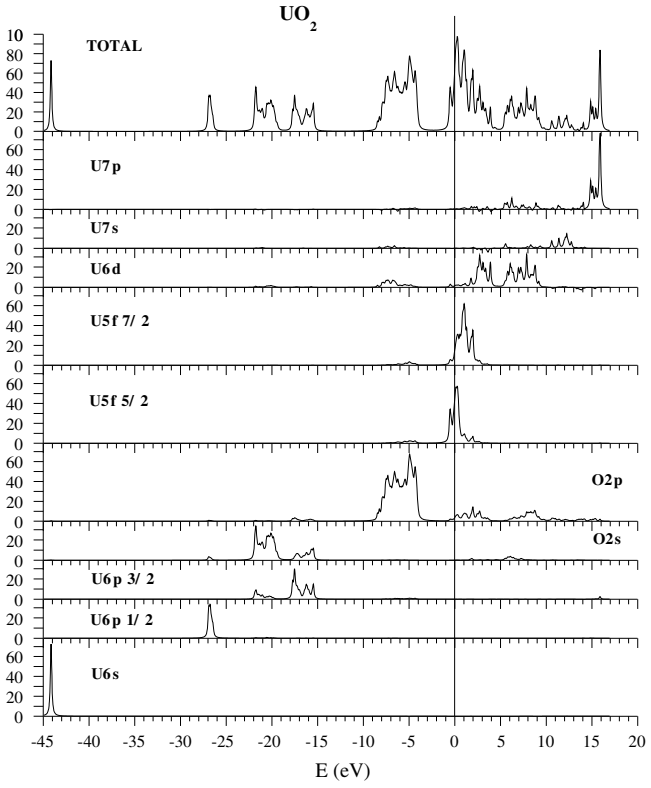

Fig. 2. Total and partial densities of states for the central part of $U_{63}O_{216}$ cluster in UO_2.

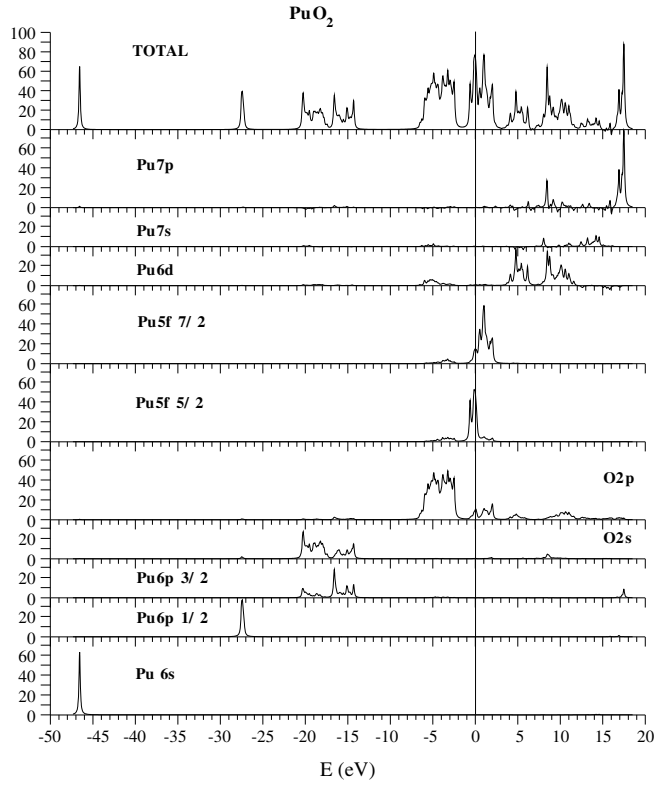

Fig. 3. Total and partial densities of states for the central part of $Pu_{63}O_{216}$ cluster in PuO_2.

conduction bands in the methods using periodic boundary conditions.

The increase of 5f states occupation on going from UO_2 to PuO_2 shifts the Pu5f levels downward to O2p band (Fig. 3). Though the energy gaps between O2p and Ac6d sates are close in both oxides, the Pu6d band position measured relative to E_F (which is used as a zero of energy scale) is shifted upward by ~2 eV. The $Pu6p^{3/2}$–O2s band gap is also reduced as compared with UO_2, this shift is accompanied by the corresponding increase of $O2s–6p^{3/2}$ covalent mixing. The spin-orbital splitting of 6p states is also larger in PuO_2.

For the evaluation of direct and indirect relativistic effects we have made the non-relativistic spin-unrestricted DV calculation of $U_{63}O_{216}$ cluster with the same computational parameters as in RDV approach. Though the detailed features of the bands in DV and RDV approaches are different, the band widths of O2p, U5f, 6d and 7p states are quite similar in both methods. The principle difference is revealed for the U6s and U6p–O2s bands. The relativistic contraction of U6s MOs decreases their energy by 17 eV. In the case of U6p–O2s states the simple non-relativistic two-band (U6p and O2s) structure transforms to the three main bands due to the spin-orbital interaction (Fig. 2). The latter result is in agreement with the experimental photoelectron spectra of UO_2 [20].

On the other hand, the considerable relativistic transformation of the core and semicore states could lead to the change in nucleus screening and, therefore, to the additional transformation of the structure of valence orbitals. In the case of UO_2 these indirect relativistic effects induce the decrease of O2p–U6d band gap by 1.5 eV and the change of the degree of U5f states delocalization. The latter could be evaluated by the values of overlap populations (n_{ij}) of various pairs of the metal and ligand atomic orbitals, which can also give the bond orders of these states [21]. The values of n_{ij} for O2p and 6d, 5f, 7s, 7p AOs of U and Pu obtained in DV and RDV calculations are listed in Table 1. Examination of Table 1 reveals that Ac5d orbitals play the main role in chemical bonding of dioxides and their contributions are nearly identical in the relativistic and non-relativistic description. On the contrary, the overlap populations of U5f–O2p states increase by 1/3 on going from DV to RDV approach. It can be seen that U5f contribution to bonding is only 2.5 times less than that of the main U6d–O2p interaction in the fully relativistic description. The Pu5f–O2p bonding in PuO_2 is even stronger, as compared with UO_2. However, the most prominent role of the indirect relativistic effects is detected for Ac7s orbitals, the corresponding relativistic values of the overlap populations are almost two times greater than those in the non-relativistic calculations. The anti-bonding character of Ac7p–O2p AOs interaction is rather unexpected result, because in the non-relativistic description their contribution to chemical bonding is usually positive, as well as those of the similar 6p states of lanthanides [22].

Table 2 lists the effective charges on atoms obtained in DV and RDV calculations for the main part of $Ac_{63}O_{216}$ clusters in UO_2 and PuO_2. A comparison of the Q_{eff} in Table 2 with the Mulliken values shows that the latter are nearly three times less than the integral charges. Though the Q_{eff} obtained by spatial integration are always more realistic than the Mulliken and Hirshfeld values [19,23], the charges on uranium, plutonium and oxygen atoms are noticeably less than their formal valencies in dioxides. The decrease of the effective charges on going from UO_2 to PuO_2 is mainly due to the increase of O2p–Ac5f covalent mixing which is the result of the smaller splitting of corresponding bands in PuO_2 (Fig. 3). The same effect is found for UO_2 where the lowering of O2p–U5f band gap by 1 eV in DV approach (with corresponding increase of covalent mixing) reduces the charges on uranium atoms by 20%, as compared with RDV calculations. In the cluster models of the periodic systems one could not simply define the so-called formula unit, and thus the effective charges obtained in this approach could not provide the electroneutrality condition for the selected group of atoms. In the case of relativistic calculation of UO_2 the total charge, $Q_{U1} + 2Q_{O1} = -0.07$ is found to be noticeably less than that in the non-relativistic approach (−0.39) and in RDV calculation of PuO_2: $Q_{Pu1} + 2Q_{O1} = -0.22$. As mentioned in Ref. [19], the charge balance is better for the compounds with wider gap between metal and

Table 1
Overlap populations of U_1, Pu_1 6d, 5f, 7s, 7p and $O_1$2p orbitals (the sum for $2p^{1/2}$ and $2p^{3/2}$ AO) in UO_2 and PuO_2 (10^{-3} e, per one ligand).

AO	UO_2		PuO_2
	DV	RDV	
$Ac6d^{3/2}$–O2p	168	67	66
$Ac6d^{5/2}$–O2p		99	97
$Ac5f^{5/2}$–O2p	48	25	18
$Ac5f^{7/2}$–O2p		39	53
Ac7s–O2p	31	55	59
$Ac7p^{1/2}$–O2p	9	9	2
$Ac7p^{3/2}$–O2p		−25	−54

Table 2
Effective charges on atoms in UO_2 and PuO_2 obtained by spatial integration [19] and Mulliken population analysis in RDV and DV calculations.

Atom	UO_2				PuO_2	
	DV		RDV			
	Integral	Mulliken	Integral	Mulliken	Integral	Mulliken
$U_1(Pu_1)$	2.45	1.25	2.97	1.04	2.46	0.77
O_1	−1.42	−0.59	−1.52	−0.51	−1.34	−0.39
$U_2(Pu_2)$	2.43	1.14	2.94	1.00	2.50	0.79
O_2	−1.42	−0.60	−1.53	−0.51	−1.34	−0.39
O_3	−1.42	−0.60	−1.52	−0.51	−1.34	−0.39

ligand valence bands (in the case of wide gap insulators CaF_2 and SrF_2 these values are within 0.02).

In $U_{63}O_{216}$ cluster the highest occupied (HOMO) and the lowest unoccupied (LUMO) molecular orbitals correspond to Γ_6^+ and Γ_6^- irreducible representations, respectively. The HOMO contains more than 50% of $5f^{5/2}$ atomic orbitals of U_3 with admixtures of $U_2 5f^{5/2}$ and $O_1 2p$, $O_2 2p$ character; the LUMO is also of the $U_3 5f^{5/2}$ character. Noticeable admixtures of the $U_1 5f^{5/2}$ and $U_2 5f^{5/2}$ states appear in MOs just below E_F, however, the molecular levels with considerable $U_1 5f^{5/2}$ and $U_2 5f^{5/2}$ contributions are located ~0.5 eV and 0.45 eV below the HOMO. Unoccupied orbitals containing the main contributions of $U_1 5f^{5/2}$ and $U_2 5f^{5/2}$ AOs begin at 0.1 eV and 0.05 eV above the LUMO. Thus according to the ground state calculation of 279-atom cluster the energy difference for the $5f^{5/2}$ electron transition from U_1 to U_2 (or in the opposite direction) is equal or greater than 0.5 eV. In $Pu_{63}O_{216}$ cluster the HOMO and LUMO correspond to Γ_6^- and Γ_7^- representations and also do not contain any noticeable contributions of the $Pu_1 5f^{5/2}$ states. However, in this cluster the Fermi level is located just above the main peak of $Pu_1 5f^{5/2}$ DOS (Fig. 3) and the energy of the highest occupied level belonging to $Pu_1 5f^{5/2}$ orbital is only 0.03 eV less than that of the LUMO (corresponding to $Pu_3 5f^{5/2}$ character). Unoccupied orbitals of $Pu_2 5f^{5/2}$ character begin at 0.02 eV above the LUMO and therefore the energy edge for the electron transition from Pu_1 to Pu_2 is essentially lower than in $U_{63}O_{216}$.

For the investigation of the effects of electronic structure relaxation following the $5f^{5/2}$ electron transition between two individual actinide atoms in the dioxide lattice, the RDV calculations of $Ac_{13}O_{56}$ clusters with C_{2v} symmetry were carried out. The total and partial DOS obtained for the central U_1 and O_1 atoms in the ground state calculations of $U_{13}O_{56}$ cluster are shown in Fig. 4. Though some details of the valence bands shape are different for 279- and 69-atom fragments, the positions and widths of O2s–Ac6p and O2p–Ac5f, 6d states are surprisingly very close in both models. However, the Ac7s and 7p orbitals appeared to be sensitive to the cluster size, in small fragments the main peaks of U(Pu)7s and 7p DOS shift downward about 2 eV and 3 eV, respectively in both oxides. The contributions of $5f^{5/2}$ AOs of the central atom in

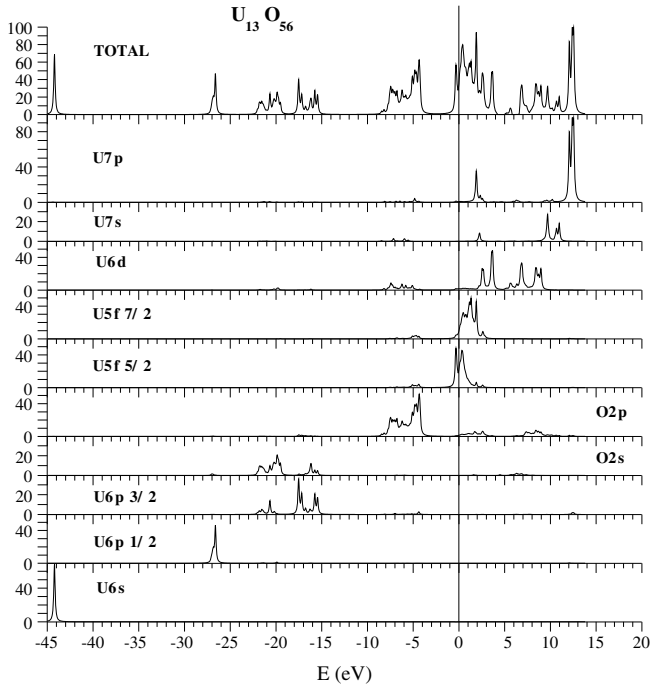

Fig. 4. Total and partial densities of states for the central part of $U_{13}O_{56}$ cluster in UO_2.

the HOMO and LUMO are also small as in the calculations of large clusters. Note that 12 atoms of U(Pu)$_2$ type (Fig. 1) become non-equivalent in $Ac_{13}O_{56}$ model and form five types of symmetrically equivalent centers: $Ac_2^{(1)}$ and $Ac_2^{(2)}$ along the new z axis, $4Ac_2^{(3)}$, $2Ac_2^{(4)}$ and $4Ac_2^{(5)}$ in the planes which are perpendicular to this axis. The analysis of possible electron transitions between MO levels corresponding to $Ac_1 5f^{5/2}$ and $Ac_2^{(1)} 5f^{5/2}$ character showed that in the ground state calculation of $U_{13}O_{56}$ the energy difference of such transitions is equal or greater than 0.5 eV, i.e. is close to the value obtained for the transition from U_1 to the $5f^{5/2}$ states delocalized among 12 equivalent U_2 centers in $U_{63}O_{216}$. In the case of the ground state calculation of $Pu_{13}O_{56}$ cluster the energy of the transition from occupied $Pu_1 5f^{5/2}$ to vacant $Pu_2^{(1)} 5f^{5/2}$ levels is near 0.2 eV, i.e. this value is greater than 0.05 eV obtained for the $Pu_{63}O_{216}$ cluster.

The transition state calculations were started from the direct changing of the population of $Ac_1 5f^{5/2}$ and $Ac_2^{(1)} 5f^{5/2}$ basis atomic orbitals by −0.5 and +0.5, respectively. As a result the energy difference of the molecular orbitals of $Ac_1 5f^{5/2}$ and $Ac_2^{(1)} 5f^{5/2}$ character achieved ~13 eV in both oxides. This result means that the electron transition between MOs with 100% contribution of $Ac_1 5f^{5/2}$ and $Ac_2^{(1)} 5f^{5/2}$ AOs without admixtures of any other orbitals could be possible with the excitation energy near 13 eV. However, there are no such $5f^{5/2}$ molecular states "purely" located on an individual metal site in $Ac_{13}O_{56}$ clusters as well as in $Ac_{63}O_{216}$ clusters. Actually the half of the hole and the half of additional electron are partially distributed over the nearest neighbors and next nearest neighbors and during self-consistency the configurations of several atoms are modified. As a result the energy difference between initial and final molecular levels converged to the values which are near 1.0 eV and 0.9 eV in $U_{13}O_{56}$ and $Pu_{13}O_{56}$ clusters, respectively. Thus the results of our calculations show that these values are strongly connected with the covalency effects in the electronic structure and could also be considered as some indirect measure of the degree of $5f^{5/2}$ states hybridization in uranium and plutonium dioxides.

In LDA + U studies the U values are usually found empirically, however in the paper of Anisimov and Gunnarsson [24] the first-principles procedure for the calculation of U was described. In order to compute this parameter, one has to remove the transfer integrals between the f orbitals and the rest of the system and the occupancy of the f orbitals of the nearest metal sires is varied, while the other metal electrons are allowed to relax self-consistently, and it follows that the "screened" $U = E(f^{n+1}) + E(f^{n-1}) - 2E(f^n)$, where E is the LDA total energy. In the case of dioxides the hybridization of metal and oxygen orbitals noticeably decreases the band gap as compared with the value of U. For instance, Lasowski et al. [5] used $U = 0.4$ Ry to obtain the experimental gap of about 2 eV in UO_2. In our calculations the above mentioned value of 13 eV (near 1 Ry) means the energy difference without any "screening" and the final self-consistent values of 1.0 and 0.9 eV include the effects of relaxation of all metal and ligand states.

4. Conclusions

Our investigations of the uranium and plutonium dioxides confirm the earlier results that the 5f states of metal atom are strongly hybridized with 2p orbitals of nearest ligands as well as with 5f AOs of the next nearest neighbors and with even more distant sites. Due to this hybridization the energy difference for the transition between occupied and vacant $5f^{5/2}$ MOs located on different atoms is considerably less than 13 eV for the completely localized $5f^{5/2}$ states.

Though there were successful attempts to explain the experimental band gap in the ground state calculations, the excitation of conductivity in UO_2 and PuO_2 is an interesting phenomenon

for the theoretical investigations. According to our transition state calculations the energy differences for the initial and final levels are two times less than experimental excitation energy for both oxides. However, two metal sites participating in this process are not nearest neighbors and the $5f^{5/2}$–$5f^{5/2}$ transition corresponds to the so-called "hoping" conductivity. There is no doubt that an additional effect of the energy barriers for the electron hoping has to be considered for such excitation. The results obtained here show that a "proper" explanation of the experimental values will have to take account of both effects.

Acknowledgments

We would like to thank V.I. Anisimov for helpful discussions.

This work was supported by the Russian Foundation for Basic Research, Grant 06-08-00808.

References

[1] V.A. Gubanov, A. Rosen, D.E. Ellis, J. Phys. Chem. Solids 40 (1978) 17.
[2] J.C. Boettger, A.K. Ray, Int. J. Quant. Chem. 80 (2000) 824.
[3] J.C. Boettger, A.K. Ray, Int. J. Quant. Chem. 90 (2002) 1470.
[4] S.L. Dudarev, D. Nguyen Manh, A.P. Sutton, Philos. Mag. B 75 (1997) 613.
[5] R. Lasowski, G.K.H. Madsen, P. Blaha, K. Schwarz, Phys. Rev. B 69 (2004) 140408R.
[6] I.D. Prodan, G.E. Scuseria, R.L. Martin, Phys. Rev. B 73 (2006) 045104.
[7] J. Shoenes, J. Appl. Phys. 49 (1978) 1463.
[8] C.E. McNeilly, J. Nucl. Mater. 11 (1964) 53.
[9] V.I. Anisimov, J. Zaanen, O.K. Andersen, Phys. Rev. B 44 (1991) 943.
[10] M.V. Ryzhkov, N.I. Medvedeva, V.A. Gubanov, J. Phys. Chem. Solids 56 (1995) 1231.
[11] M.V. Ryzhkov, T.A. Denisova, V.G. Zubkov, L.G. Maksimova, J. Struct. Chem. 41 (2000) 927.
[12] D.E. Ellis, G.A. Benesh, E. Byrom, Phys. Rev. B 20 (1979) 1198.
[13] J.C. Slater, K.H. Johnson, Phys. Rev. B 5 (1972) 844.
[14] A. Rosen, D.E. Ellis, J. Chem. Phys. 62 (1975) 3039.
[15] H. Adachi, Technol. Reports Osaka Univ. 27 (1977) 569.
[16] O. Gunnarsson, B.I. Lundqvist, Phys. Rev. B 13 (1976) 4274.
[17] P. Pyykko, H. Toivonen, Acta Acad. Aboensis, Ser. B 43 (1983) 1.
[18] D.A. Varshalovich, A.N. Moskalev, V.K. Khersonskii, Quantum Theory of Angular Momentum, World Scientific, Singapore, 1988.
[19] M.V. Ryzhkov, J. Struct. Chem. 39 (1998) 933.
[20] Yu.A. Teterin, A.Yu. Teterin, Russ. Chem. Rev. 73 (2004) 541.
[21] R.S. Mulliken, Ann. Rev. Phys. Chem. 29 (1978) 1.
[22] M.V. Ryzhkov, V.A. Gubanov, Yu.A. Teterin, A.S. Baev, Z. Phys. B 59 (1985) 7.
[23] M.V. Ryzhkov, A.L. Ivanovskii, B.T. Delley, Chem. Phys. Lett. 404 (2005) 400.
[24] V.I. Anisimov, O. Gunnarsson, Phys. Rev. B 43 (1991) 7570.